Scientific Reports

https://doi.org/10.1038/s41598-026-50499-x

Article in Press

Mechanical and durability performance of mortar containing biochar derived from pyrolyzed *Posidonia oceanica* leaves: a circular approach to marine biomass waste

Received: 31 December 2025

Accepted: 21 April 2026

Published online: 13 May 2026

Cite this article as: Olabimtan S.B., Mosaberpanah M.A. & Oluwole B.O. Mechanical and durability performance of mortar containing biochar derived from pyrolyzed *Posidonia oceanica* leaves: a circular approach to marine biomass waste. *Sci Rep* (2026). https://doi.org/10.1038/s41598-026-50499-x

Stephen Babajide Olabimtan, Mohammad Ali Mosaberpanah & Babatunde Olufunso Oluwole

Mechanical and Durability Performance of Mortar Containing Biochar Derived from Pyrolyzed *Posidonia oceanica* Leaves: A Circular Approach to Marine Biomass Waste

Stephen Babajide Olabimtan[1*]; Mohammad Ali Mosaberpanah[1]; Babatunde Olufunso Oluwole[1]

Civil Engineering Department, Cyprus International University, North Cyprus, Nicosia 99258, Turkey

Corresponding author stephenbabajide1@gmail.com

ABSTRACT

This study investigates the feasibility of using biochar derived from pyrolyzed *Posidonia oceanica* leaves (PBC) as a partial cement replacement for sustainable mortar production. The research addresses two critical challenges simultaneously: valorization of marine biomass waste and reduction of the carbon footprint associated with Portland cement. Biochar produced at 400 °C was incorporated at replacement levels of 1–6 % by weight of cement, and the resulting mortars were evaluated for fresh properties, mechanical performance, durability, microstructure, and environmental impact. Workability decreased with increasing PBC content, while compressive strength at 28 days improved at low replacement levels, reaching an optimum at 3 % with 8.71 % strength increase relative to the control mixture. Water absorption decreased marginally from 5.38 % in the control to 5.31 % at optimal PBC content, but increased progressively at higher replacement levels, reaching up to 7.50 %, indicating improved matrix compactness. Higher dosages resulted in strength reduction due to increased porosity and interfacial defects. Thermal resistance testing showed stability of PBC3 specimens up to 600 °C, whereas higher contents led to structural degradation, showing microcracking and mass loss exceeding 7%. Microstructural analysis confirmed pore refinement at low dosages and matrix disruption at higher contents. Embodied carbon decreased linearly with increasing PBC content, achieving a 5.3 % reduction at 6 % replacement. One-way ANOVA confirmed that PBC dosage significantly influenced the fresh, mechanical, and durability properties of the mortar ($p < 0.05$). Overall, 3 % PBC was identified as the optimal dosage balancing mechanical performance, durability, and sustainability. The findings position biochar as a sustainable solution for lowering cement consumption and transforming PBC waste into value-added construction materials.

Keywords: Biochar; Cementitious materials; Fresh and hardened properties; Posidonia Oceanic leaves; Sustainable waste

1. INTRODUCTION

Portland cement production remains one of the most carbon-intensive industrial processes, contributing between 5 and 8% of global CO_2 emissions (Nejad et al 2025). Although advancements in manufacturing techniques and the development of alternative materials have been made, the surging global demand for cementitious composites, driven by rapid urbanization and industrial expansion, continues to exert considerable pressure on natural resources and the environment (Bărbulescu & Hosen, 2025). In response to the increasing scarcity of natural resources and the significant environmental burden associated with Ordinary Portland Cement (OPC) production, research efforts have increasingly focused

on partially replacing OPC with supplementary cementitious materials (SCMs). These include industrial byproducts such as rice husk ash; silica fume, waste glass powder and marble or granite dust (Olii et al 2025; Gunasekaran et al 2024; Oluwole et al 2025; Liu et al 2025; Babajide & Mosaberpanah 2023; Danish et al 2021; Olabimtan et al 2023). These waste materials are generated in large and growing quantities from various industrial processes. Traditional disposal methods have led to adverse environmental and economic consequences, emphasizing the necessity for more sustainable waste management strategies.

Biochar (BC) is a carbon-rich material produced from lignocellulosic biomass under oxygen-limited conditions. When derived from saccharification residues, it can reduce CO_2 emissions by about 67% compared to rice straw burning, demonstrating significant environmental sustainability potential (Chaturvedi et al., 2024). BC has many benefits, including carbon dioxide sequestration, soil amendment pollution absorption and others (Kushwah, et al 2024; Shyam et al 2025; Gupta et al 2018; Mosaberpanah et al 2024).

According to the International Biochar Initiative, biochar is the solid material created by carbonizing biomass. This is achieved through a process of thermochemical decomposition (pyrolysis) at temperatures between 450–550 °C in an oxygen-free atmosphere (Chaturvedi et al 2024). From an environmental perspective, incorporating biochar into construction materials not only facilitates carbon sequestration within structures for a prolonged duration but also contributes to maintaining a balance in global carbon cycles. Extensive literature has delved into the use of biochar in cementitious materials, with a focus on its role as a filler (Gupta, et al 2021; Sirico et al 2020; Tan et al 2020). The inclusion of biochar as a filler has been shown to alter the mechanical and physical properties of cement composites (Akinyemi et al 2020; Olabimtan et al 2025; Mohammad et al 2024). Biochar is mainly produced by pyrolysis, a process that heats biomass with little or no oxygen. Slow pyrolysis yields more char, while fast pyrolysis produces biochar with a higher surface area (Kumar et al., 2021; Zeidabadi et al., 2018).

Based on a review of a range of testing results from different studies of biochar, it can be concluded that workability decreases as the biochar replacement ratio increases (Yang et al 2021; Danish et al 2021; Muthukrishnan et al 2019). According to Suarez-Riera et al (2020), they investigated using wood chips and biochar in place of cement in mortar. They discovered that 2% biochar served as a micro-reinforcement, increasing flexural strength by 15%. Another researcher, Aneja et al (2022) found that the inclusion of 4% biochar in concrete boosted compressive strength by 2.32%, flexural strength by 23.52%, and durability by 17.3%. The finer biochar particles played a key role in creating a denser matrix, accounting for these improvements (Singhal, S. 2023).

Qin et al. (2021) reported that incorporating biochar in pervious concrete up to 13.5% improved mechanical strength, with optimal performance at 6.5% replacement while maintaining permeability. Recent studies further demonstrate biochar's effectiveness in cementitious systems, showing that biomass-derived biochar can enhance strength, durability, and microstructural densification while reducing cement demand and associated emissions. Its porous structure promotes internal curing and improved matrix integrity, reinforcing its potential as a sustainable additive for low-carbon construction materials (Patel et al 2025; Murali et al 2026).

In the pursuit of a circular economy, researchers have proposed using *Posidonia oceanica waste* as a viable secondary raw material to substitute for wood-based panels (Cocozza et al 2011). Its leaves have also been reported to aid soil stabilization, reduce coastal erosion, and serve as materials for artisanal applications (Malekzadeh & Bilsel 2014). The potential for using *Posidonia oceanica* fibres in composite materials was first suggested by Ben Hadj et al (2024), who noted their favorable thermal and acoustic properties when enhanced by chemical treatments, suggesting their viability for integration into composite materials. This spurred investigations into suitable binders, with a focus on sustainable and bio-based composites. Kuqo et al. (2018) investigated this approach and found that the fibres improved thermal and acoustic characteristics, reporting a relative increase in compressive strength. However, subsequent findings have highlighted a critical trade-off. At high concentrations of 40%, *Posidonia* fibres were shown to severely degrade mechanical performance, reducing both compressive and flexural strength using a 0.50 water/cement ratio discovered that a 10% addition of *Posidonia* fibres yielded the optimal compressive strength of 33.60 MPa. In contrast, research focusing on lower dosages found more positive outcomes. Hamdaoui et al. (2018) evaluated hardened cement paste containing 5–20% Posidonia oceanica by volume and reported that its incorporation enhanced both thermal insulation performance and mechanical properties, including compressive strength and toughness.

Recent studies have demonstrated that the performance of cementitious composites can be enhanced through advanced modification strategies such as nanomaterial incorporation, fiber reinforcement, and alternative binder systems. For instance, nano-engineered additives and dispersion techniques have been shown to improve hydration kinetics, microstructure, and strength development, while fiber and fabric reinforcements enhance ductility and crack resistance. Similarly, alkali-activated and lightweight composite systems have exhibited improved thermal stability, structural performance, and sustainability potential (El-Feky & El-Rayes, 2019; Nazar, et al 2020; Amer et al., 2025; Hamed et al., 2024). In Parallel to this, *Posidonia oceanica leaf* biochar (PBC) produced through photosynthesis from carbon dioxide and water, represents the sole renewable resource for energy and chemical feedstock generation (Makepa et al 2025). Thus, this research centres on using Pyrolysed *Posidonia oceanica Leaf* waste biochar as a cement replacement in mortar production.

Although previous studies have explored the incorporation of biochar in cement-based materials, a systematic and comprehensive evaluation of pyrolyzed PBC on the fresh, mechanical, durability, and microstructural performance of cementitious composites remains limited. Existing research has primarily focused on isolated properties or specific applications, without providing an integrated assessment of performance, sustainability, and material behavior. Moreover, the mechanisms governing the interaction between PBC particles and the cement matrix, particularly at varying replacement levels, are not yet fully understood. Therefore, a detailed investigation is required to clarify the multifunctional role of PBC and to determine its optimal dosage for enhancing performance while reducing environmental impact.

In response to environmental concerns associated with CO_2 emissions from cement production, this study aims to: (1) evaluate the pozzolanic potential of biochar, (2) assess its influence on mortar strength while maintaining structural performance, (3) determine the optimum cement replacement level using marine biomass-derived biochar, and (4) compare the performance of mixtures containing varying proportions of PBC with

conventional mortar. Accordingly, a comprehensive evaluation of its effects on key performance indicators, including mechanical strength, durability, and resistance to chemical and thermal exposure, is analyzed.

2. MATERIALS and METHODS

2.1 Raw Materials

2.1.1 Collection and preparation of biochar

The biomass selected for biochar production was derived from leaves of *Posidonia oceanica, a* seagrass endemic to the Mediterranean Sea. The material was collected from the Iskele long beach, North Cyprus. This biomass is considered marine waste and is freely accessible in the public domain. No live plants were collected, and no protected or endangered species were affected. In accordance with local environmental regulations, no specific permits or licenses were required for the collection of this material. As the study utilized degraded beach-cast leaf residues, the deposition of voucher specimens in a public herbarium was not applicable. The raw leaves were presoaked, thoroughly washed, and rinsed with tap water to eliminate sand, shells, and other debris. Following the washing process, the leaves were air-dried at ambient temperature to remove surface moisture, then subsequently oven-dried at 105°C for 24 hours to ensure complete moisture removal.

2.1.2 Pyrolysis Process and Biochar Production

The dried *Posidonia oceanica* leaves were subjected to slow pyrolysis in a muffle furnace according to the procedure outlined in ASTM D3174-12. The pyrolysis was conducted at a heating rate of 10°C per minute, reaching a final temperature of 400°C, which was maintained for one hour which generally results in predominantly amorphous carbon with limited graphitic ordering; thus, its influence on cementitious performance mainly by physical characteristics such as porosity, surface area, and morphology. A slow heating rate was deliberately employed to reduce char flammability and maximize biochar yield. Pyrolysis was carried out in an oxygen-limited environment within the furnace chamber to prevent combustion during carbonization. Upon completion of thermal decomposition, the carbonized material underwent controlled temperature reduction within the heating chamber until it attained room temperature resulting biochar was then mechanically ground and sieved through a 75 µm sieve to obtain a fine powder suitable for incorporation into cement mortar. The resulting *Posidonia* biochar yield (YPBC), calculated as the mass ratio of the char obtained to the original dry biomass, and was approximately 25 wt%. The processing of Posidonia leaf-based biochar is seen in **Figure 1.**

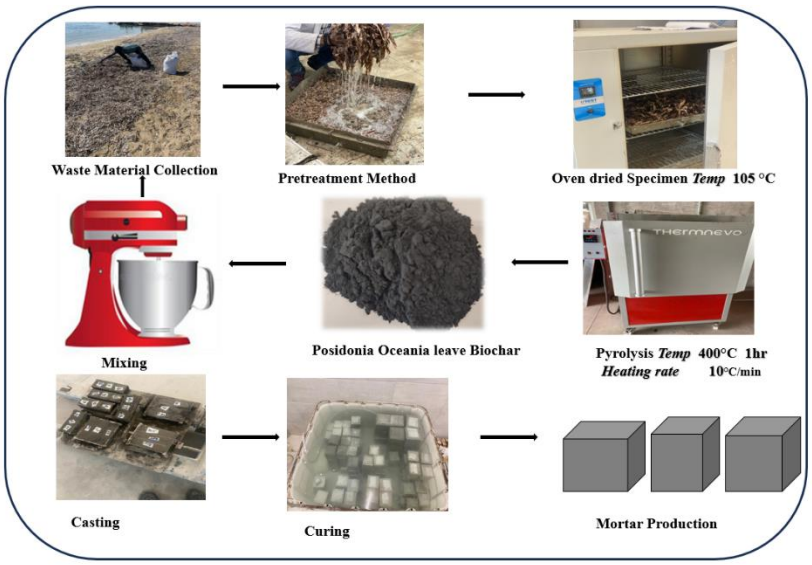

Figure 1: Production workflow of *Posidonia oceanica* biochar showing the sequential steps of collection, washing, drying, and pyrolysis at 400°C for 1 hour**.**

2.1.3 Characterization of Posidonia oceanica Biochar

The particle size distribution of the biochar was analyzed using a laser diffraction particle size analyzer (Mastersizer 3000) under wet dispersion conditions. As illustrated in **Figure 2**, the particle size distribution of the ground biochar ranged predominantly from 1 to 100 µm. The cumulative distribution revealed that approximately 75% of the biochar particles were finer than 30 µm, while 50% were below 10 µm (D_{50} = 10 µm). Notably, a substantial fraction of the biochar particles exhibited a finer particle size than typical cement, which has a median particle size of approximately 15-20 µm. This fine particle size distribution is advantageous for the filler effect and may enhance the pozzolanic reactivity of the biochar. The specific surface area, micropore size, and pore volume of the produced (PBC) were determined using the Brunauer-Emmett-Teller (BET) method with N_2 adsorption (Quantachrome instrument). Before analysis, PBC samples (0.18 g) were degassed at 120°C for 8 hours to remove adsorbed gases and moisture. **Table 1** presents the physical characteristics of the PBC.

Table 1. Outline of the Physical Properties of the Biochar

Physical properties	Biochar
Specific Gravity	1.69
Bulk Density ρ (g·cm^{-3})	0.35
Water Absorption %	118
Length	150mm
Width	10mm
pH	8.5
Particle size	75µm
% Yield of biochar	25%
% Ash	16.34
Specific surface Area (BET)	1253m^2/g
Colour	Black

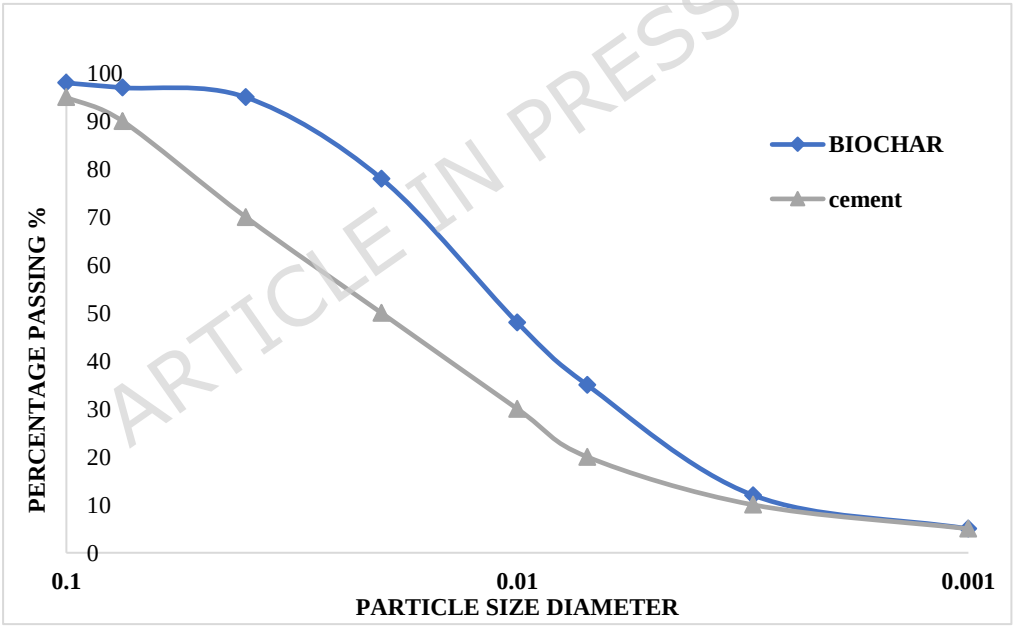

Figure 2: Particle size distribution of the materials

2.1.4 Fine Aggregate

Within cementitious composites, the essential role of fine aggregate is to fill the interstitial spaces among larger aggregate particles. The American Society for Testing and Materials standard ASTM C33/C33M-18 establishes the criteria for fine aggregate gradation and quality, encompassing acceptable particle size ranges and allowable contaminant levels for materials such as natural river sand. For the present investigation, crushed limestone powder served as the fine aggregate component. The detailed specifications of this material are presented in **Table 2**. To ensure compliance

with the particle size distribution requirements specified in ASTM C136/C136M-19, the crushed limestone sand was mechanically sieved, as demonstrated in **Figure 3**. Furthermore, in accordance with the procedures outlined in ASTM C128-15, the fine aggregate was conditioned to a saturated surface-dry state before mixing. This conditioning step was implemented to prevent the aggregate from absorbing additional water during the mixing phase, thereby maintaining the intended water-to-binder ratio.

Table 2. Properties of fine aggregate.

Physical Properties	Value
Specific Gravity	2.63
Moisture absorption (%)	1.32
Bulk density (kg/m³)	1728
Loss bulk density (kg/m³)	1576
Fineness modulus	2.79
Moisture content (%)	0.1

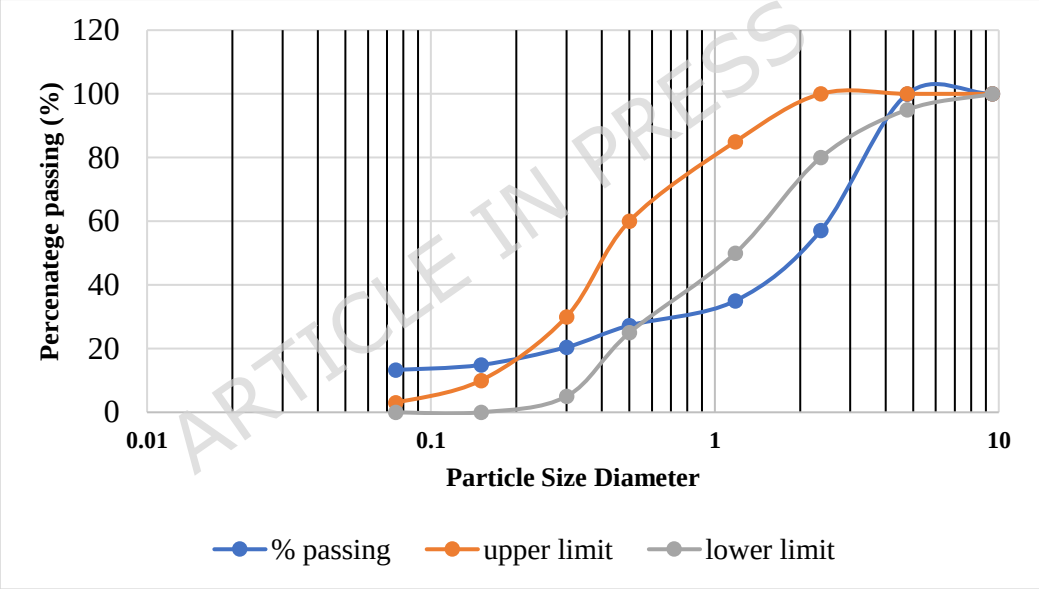

Figure 3: Sand grain gradation.

2.1.5 Cement

The binder employed in this investigation was CEM I 42.5 Ordinary Portland Cement (OPC), conforming to the specifications outlined in ASTM C150/C150M-21 and TS EN 197-1. The cement was procured from ÇİMSA Çimento San. ve Tic. A.Ş., a manufacturing facility located in Mersin, North Cyprus. This grade of cement is widely utilized in diverse construction applications, encompassing mortar production, plastering, screeding, surface coatings, and thermal insulation systems. The resulting chemical composition data are presented in **Table 3**.

Table 3: Chemical characterization of Cement and Posidonia Oceania Biochar

Chemical Compound	Cement	Posidonia oceanica Biochar
CaO	56	45.6
SiO_2	17	3.25
Al_2O_3	5.50	2.62
Fe_2O_3	3.0	2.49
SO_3	3.0	1.37
K_2O	0.9	1.84
Na_2O	0.4	0.9
TiO_2	-	0.06
MgO	2.5	5.07
MnO	-	0.10
Cr_2O_3	-	0.023
LOI	-	36.6
Insoluble Residue	2.0–5.0	-
C	-	58.72
N	-	0.85
H	-	6.15
O	-	33.64

2.1.6 Water

Potable tap water with a neutral pH ranging from 6.5 to 7.0 was employed for all mixing operations. The water was devoid of acidic compounds, organic contaminants, oils, and other deleterious substances that could adversely affect cement hydration.

2.1.7 Superplasticizer

A polycarboxylate-ether-based high-performance water reducer (CHRYSO Fluid Premia 196) was employed to enhance workability. This admixture, procured from CHRYSO S.A.S., exhibited the following characteristics: density of 1.055 ± 0.01 g/cm³ at 20°C, pH value of 7.50 ± 2.00, solid content of 25.00 ± 1.20% (determined by halogen analysis), sodium oxide equivalent not exceeding 1.50%, and chloride ion content below 0.10%.

2.2 Method

2.2.1 Mortar Specimen Preparation

Mortar specimens were prepared using a standardized mix design with a binder-to-sand-to-water mass ratio of 1:2.25:0.35. The binder component consisted of OPC and PBC in varying proportions. Mixing was conducted in accordance with ASTM C305-20 using an automatic programmable mortar mixer (UTCM-0885E) at ambient temperature. The mixing procedure consists of the following steps: (1) dry blending of sand, cement, and biochar for one minute to ensure uniform distribution; (2) addition of approximately 70% of the mixing water followed by two minutes of mixing at moderate speed to achieve initial homogenization; (3) incorporation of the remaining water (pre-mixed with the superplasticizer) and continued mixing for an additional two minutes; (4) a one-minute rest period to allow for particle wetting; (5) scraping of the mixer bowl edges to incorporate any unmixed material; (6) high-speed mixing for 30 seconds to ensure complete dispersion; and (7) final mixing at moderate speed for one minute. The workability of each mix was assessed using the flow table test according to ASTM C1437-15. Following mixing, the fresh mortar was vibrated on a vibrating table for one minute to eliminate entrapped air voids. The mortar was then cast into moulds of various dimensions: 50×50×50 mm cubes for compressive strength and durability testing, 40×40×160 mm prisms for flexural strength determination, and 25×25×285 mm beams for drying shrinkage measurements. The filled molds were covered with polyethylene film to prevent moisture loss and allowed to set for 24 hours at room temperature. After demolding, all specimens were transferred to a water-curing tank maintained at 23±2°C. Specimens were cured for 7 and 28 days, prior to testing for mechanical properties (compressive and flexural strength) and durability characteristics (water absorption, acid resistance, and fire resistance).

2.2.2 Mix design

To systematically evaluate the influence of PBC on mortar properties, seven distinct mortar mix proportions were formulated, as summarized in **Table 4.** The experimental program comprised a reference mortar (CM) with no cement replacement, and six biochar-enhanced mortars designated PBC1, PBC2, PBC3, PBC4, PBC5, and PBC6. These mixes incorporated biochar as a partial cement substitute at dosages of 1%, 2%, 3%, 4%, 5%, and 6% by mass, respectively. The nomenclature system adopted reflects the biochar content, with the numeric suffix indicating the approximate replacement percentage. The binder component consisted of cement and biochar, maintaining a constant total binder content across all mixes. To ensure adequate workability, a polycarboxylate-based superplasticizer was incorporated at a dosage of 1.05% by mass of the total binder content, which remained consistent across all mix designs. For each mix proportion, three cube specimens were cast and tested, and the reported results represent the average of the three specimens.

Table 4: Mix proportion of mortar specimens

Mix ID	C	PBC	W/B	Cement (g)	PBC (g)	Sand (g)	Water (g)	SP (wt % of binder)
CM	100	0	0.35	684.00	0	1538	239	1.05
PBC_1	99	1	0.35	677.16	6.84	1538	239	1.05

PBC_2	98	2	0.35	670.32	13.68	1538	239	1.05
PBC_3	97	3	0.35	663.48	20.52	1538	239	1.05
PBC_4	96	4	0.35	656.64	27.36	1538	239	1.05
PBC_5	95	5	0.35	649.8	34.2	1538	239	1.05
PBC_6	94	6	0.35	642.96	41.04	1538	239	1.05

2.2.3 Curing

Following a 24-hour initial setting period, specimens were demolded and subjected to controlled curing conditions to facilitate proper hydration and strength development. Water curing was conducted by immersing the specimens in a temperature-controlled water bath maintained at 20±2°C. Specimens were retrieved from the curing tank at predetermined ages of 7 and 28 days for mechanical and durability testing. The various curing conditions employed in this study are illustrated in **Figure 4**.

Figure 4. Specimen curing and conditioning procedure.

2.2.4 Workability

The workability of the fresh mortar was evaluated using the flow table test in accordance with ASTM C1437-15. This test measures the consistency and spread diameter of the mortar under standardized conditions.

2.2.5 Water Absorption

Water absorption testing is a critical durability assessment for cementitious composites, as it provides insight into the porosity and permeability of the hardened matrix. The test was conducted in accordance with ASTM C642-21 to quantify the volume of permeable voids and the material's capacity to absorb water under specified conditions

2.2.6 Compressive Strength

The compressive strength of the biochar-modified mortar specimens was evaluated in accordance with ASTM C109/C109M-20a. Testing was performed using a universal compression testing machine on 50×50×50 mm cubic specimens at curing ages of 7 and 28days. Three specimens were tested for each mix at each age, and the average value was reported. The test setup and representative specimens are shown in **Figure 5.**

Figure 5: Compressive and flexural strength test machine.

2.2.7 Flexural Strength

Flexural strength, which quantifies a material's resistance to bending under transverse loading, was evaluated in accordance with ASTM C348-21. Testing was performed on 40×40×160 mm prismatic specimens after 28 days of water curing using a three-point bending configuration. Each specimen was positioned on two roller supports with a span length of 120 mm, and a concentrated load was applied at mid-span at a constant rate of 2 kN/s until failure occurred. Three specimens were tested for each mix composition, and the average flexural strength was calculated. The test setup is illustrated in **Figure 6**.

Figure 6: Flexural strength test machine.

2.2.8 Density

Density is a fundamental physical property that provides insight into the compactness of the cementitious matrix and the effectiveness of pore filling by the biochar particles. The density of the mortar specimens was measured at 28 days using the buoyancy method in accordance with ASTM C567-14, with calculations performed following the procedure outlined in ASTM C642-13.

2.2.9 Drying Shrinkage

Drying shrinkage refers to the volumetric contraction of cementitious materials that occurs when internal moisture is lost under ambient conditions. This phenomenon occurs when water evaporates from the pore structure, creating capillary tension forces that draw the solid particles closer together, thereby inducing internal tensile stresses. If these stresses exceed the tensile strength of the material, cracking can occur. Drying shrinkage measurements were performed in accordance with ASTM C596-18 using a length comparator equipped with a dial gauge. Prismatic specimens (25×25×285 mm) were demolded after 24 hours and subjected to controlled drying conditions. Length change measurements were recorded at regular intervals over 28 days, and the results for all mix compositions are presented in **Figure 7**.

Figure 7. Dry shrinkage of the mixtures.

2.2.10. High temperature Resistance

The high-temperature performance of the biochar-modified mortar were evaluated using an electric muffle furnace in accordance with ASTM E119-20. This test assesses the material's ability to maintain structural integrity and resist degradation when exposed to elevated temperatures. Cubic specimens (50×50×50 mm) were subjected to three target temperatures: 200°C, 400°C, and 600°C, representing moderate, severe, and extreme fire conditions, respectively. The electric furnace used for testing is shown in **Figure 8.** After exposure, specimens were evaluated for mass loss, residual compressive strength, and visual damage to characterize their thermal stability and fire resistance.

Figure 8. An electric chamber furnace.

2.2. 11 Sulfuric acid resistance

Sulfuric acid resistance was evaluated based on visual deterioration, mass variation, and residual compressive strength following acid exposure, in accordance with procedures consistent with ASTM C267. After 28 days of water curing, specimens were removed, surface dried to a saturated surface-dry (SSD) condition, and their initial mass was recorded. The specimens were subsequently immersed in a 2% H_2SO_4 solution at room temperature for 28 days. The solution was renewed at weekly intervals to maintain a consistent acid concentration and prevent change in pH. At the end of the exposure period, specimens were removed, rinsed with distilled water to eliminate residual acid, surface dried, and reweighed. Residual compressive strength was then determined and compared with unexposed control specimens to quantify strength retention.

2.3 Microstructural Characterization

2.3.1 Scanning Electron Microscopy

The morphological features of the *Posidonia oceanica* biochar (particle size < 75 µm) were investigated using scanning electron microscopy (SEM) with a JEOL JSM-6610LV instrument (Tokyo, Japan). To ensure adequate electrical conductivity during imaging, the biochar samples were sputter-coated with a platinum-gold alloy using an SC7620 Mini Sputter Coater prior to analysis. Electron micrographs were acquired at an accelerating voltage of 30 kV. The SEM analysis, presented in **Figure 9**, revealed that PBC particles exhibited a highly irregular morphology with elongated shapes and a distinctly rough, porous surface texture. A substantial fraction of the observed pores measured less than 20 µm in diameter.

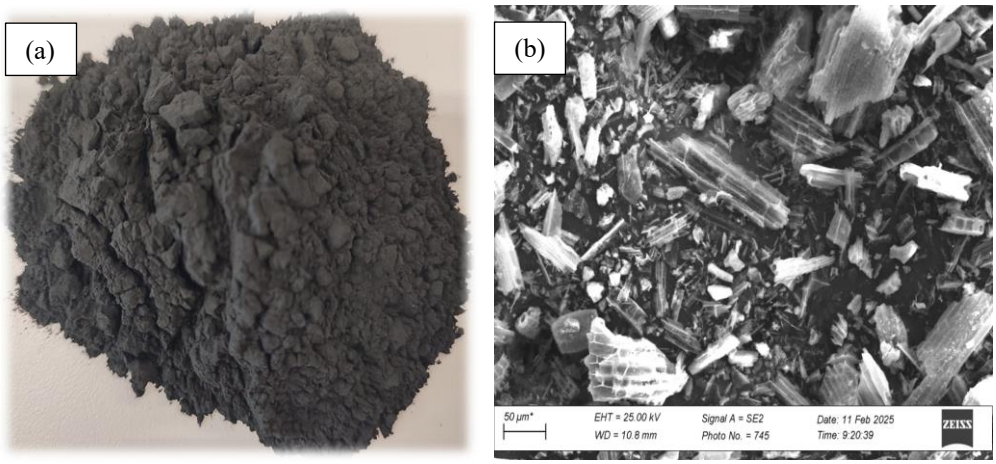

Figure 9: Morphological characterization of *Posidonia oceanica* biochar: (a) pulverized biochar powder, and (b) scanning electron micrograph showing the porous surface structure at 2,500× magnification (scale bar = 50 µm).

2.3.2 X-ray diffraction analysis and elemental composition of pyrolysed *Posidonia oceanica* biochar.

The crystalline structure of the *Posidonia oceanica* biochar was characterized using X-ray diffraction (XRD) with a Rigaku powder diffractometer equipped with Cu-Kα radiation (λ = 1.5406 Å). Diffraction patterns were collected over a 2θ angular range of 2° to 90°. As illustrated in **Figure 10,** The XRD pattern exhibited several distinct diffraction peaks superimposed on a broad diffuse hump between approximately 15° and 30° (2θ), which is characteristic of predominantly amorphous carbon structures typically observed in biochar materials. Such broad halos originate from disordered turbostratic aromatic carbon layers formed during pyrolysis . The sharp reflections were indexed to calcite ($CaCO_3$) as the main crystalline phase, with characteristic peaks detected at approximately 29.4°, 43.0°, and 57.3° (2θ), corresponding to the (104), (202), and higher-order crystallographic planes, respectively. These reflections indicate the presence of residual mineral constituents inherited from the original biomass. A minor reflection near 33.4° (2θ) may be attributed to portlandite ($Ca(OH)_2$), although its slight shift from the standard position (34.1°) suggests possible lattice distortion, limited crystallinity, or overlapping contributions from amorphous phases. Similar amorphous humps and weak crystalline peaks have been widely reported for biochar due to its predominantly non-crystalline carbon matrix (Keiluweit et al., 2010; ATEŞ, A 2025).

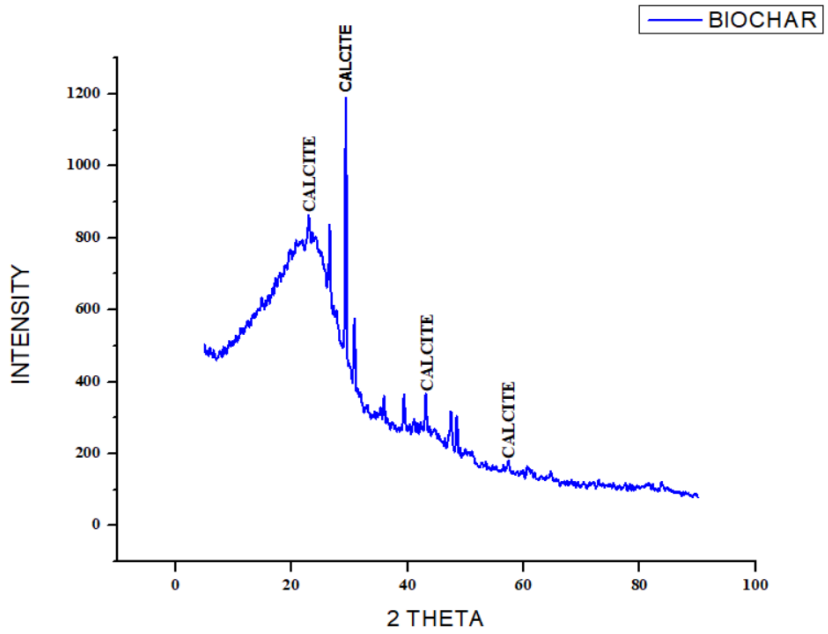

Figure 10: X-ray diffraction pattern of *Posidonia oceanica* leaf-derived biochar

2.3.3 Fourier Transform Infrared Analysis

Fourier Transform Infrared Spectroscopy (FTIR) was employed to characterize the chemical structure of PBC over the wavenumber range of 500–4000 cm^{-1}. This analytical technique operates by passing infrared radiation through the sample and recording the absorption at different wavelengths, thereby enabling the identification of functional groups and chemical bonds present in the materials (Khadir et al 2024).

2.4 Sustainability assessment

The environmental sustainability of the biochar-modified composites was assessed through quantification of embodied carbon content and eco-strength efficiency metrics, comparing PBC composites against conventional mortar systems. Embodied carbon (EC) represents the cumulative greenhouse gas (GHG) emissions arising from material, extraction, Manufacturing process, logistics, and construction assembly of cementitious composites (Chen, et al 2022). The assessment framework was conducted using a cradle-to-gate approach, covering raw material extraction, production of cementitious materials, and transportation, while excluding the use phase, construction, and end-of-life stages (e.g., demolition or recycling. In **Table 5** shows the embodied carbon emission factor for the mortar production. The EC coefficients were sourced from the Inventory of Carbon & Energy (ICE) database (Hammond, G. P., & Jones, C. I. 2008). Complementarily, the Eco-strength efficiency (ESE) serves as a sustainability indicator that evaluates the trade-off between mechanical performance (e.g., compressive strength) and environmental burden (e.g., embodied carbon) in cementitious systems. This metric facilitates comparative analysis of materials based on their structural contribution per unit of environmental impact. The computational procedures for EC and ESE determination are presented in Equations 2 and 3, respectively

$$EmbodiedCarbon\ (EC) = \sum_{a=1}^{n} (K_a \times \mathrm{CEF}a) \quad (1)$$

$$Eco - Strenght\ Efficiency\ (ESE) = \frac{\text{Compressive strength 28 days}}{Embodied\ Carbon\ emission\ proportion\ mix} \quad (2)$$

Note: Where quantity of material is (kg), emission factor (kg CO_2-eq per kg material), material type, 28 days compressive strength (MPa).

Table 5: Embodied carbon emission factors of mortar production

Materials	Carbon emission factor (CFC) ($kgCO_2/kg$)	Database
Cement	1.17	ICE
Fine aggregate	0.0195	ICE
Water	0	ICE
Biochar	0.057	Kavindi, et al 2025
Superplasticizer	0.72	ICE
Transportation	0.00441	ICE

2.5 Statistical analysis

A one-way Analysis of Variance (ANOVA) was conducted to evaluate the influence of PBC dosage (CM–PBC6) on the mechanical and durability properties of the mortar mixes. Each mix was tested in triplicate (n = 3), resulting in 21 total observations. The between-group degrees of freedom were calculated as df between = 6 (k − 1), while the within-group degrees of freedom were df within = 14 (N − k). Statistical significance was assessed at α = 0.05.

3. RESULTS and DISCUSSION

3.1 Fluidity

The flow diameter of the fresh mortar mixes containing varying proportion of PBC is shown in **Figure 11**. As the percentage of PBC decreased, there was an increased absorption of water. However, it is important to note that all mixtures exhibited reduced flowability compared to the control mix, with flow reductions ranging from 11.42% to 22.28% across the PBC content, from 1% to 6%. The lowest flow measurement was 136 mm for PBC6 mixture. The reduction in workability is primarily attributed to the porous microstructure of biochar, which absorbs mixing water and reduces the amount of free water available for lubrication and flow. As the biochar replacement level increases, the cumulative water absorption intensifies, thereby limiting the spreadability and flow characteristics of the fresh mortar (Javed, et al 2022). The porous structure created by PBC within the matrix demands extra water to ensure the mixture flows smoothly. Materials of this nature that are exposed to high temperatures tend to absorb significant amounts of water to maintain flow, preserve their shape, and prevent rapid hardening. This is why the addition of a superplasticizer was crucial in retaining the necessary water content until the samples were cast (Mosaberpanah et al 2024). PBC in mortar quickly absorbs some of the mixing water through hydrogen bonding during the preparation process, leading to a reduction in the mix's fluidity. According to Gupta et al. (2018), the large surface area of biochar necessitates the addition of extra water to improve flowability. This trend is consistent with the findings of Tan et al. (2020), who reported that higher biochar contents significantly lower flowability due to the porous structure of biochar, which tends to retain water. However, the carbon structure of PBC particles has a high cation exchange capacity (CEC),

meaning that PBC can interact with cations in the mix through ion exchange. Furthermore, the optimal biochar replacement level required to maintain adequate workability is influenced by the loss on ignition (LOI) value of the specific biochar used (Senadheera et al 2023). The primary cause of workability reduction can be attributed to the high porosity of biochar particles, which sequester mixing water within their internal pore structure during the mixing process.

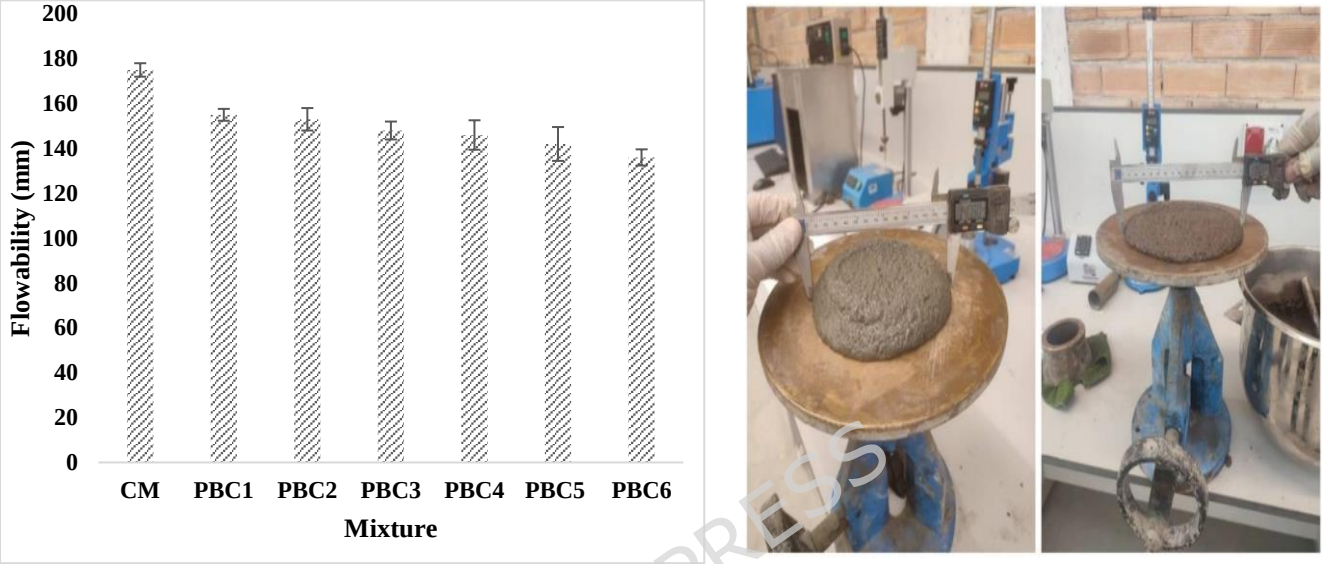

Figure 11. Flow diameter of fresh mortar mixes

The incorporation of PBC resulted in a reduction in workability compared to the control mortar, consistent with findings reported by Yang and Wang (2021) and Zhou et al. (2023), who attributed this phenomenon to the high-water absorption capacity and porous microstructure of biochar particles. However, the addition of a polycarboxylate-based superplasticizer at 1.05% by binder mass effectively compensated for this effect, maintaining adequate flow characteristics across all mix formulations and enabling proper placement and consolidation.

3.2 Fresh Density

The volumetric mass of freshly prepared mortar specimens, measured immediately following the mixing and casting operations, exhibited values ranging from 2335-2410 kg/m^3 across the experimental matrix. Analysis of the data presented in **Figure 12** reveals the fresh density mortar mixes. The progressive substitution of Portland cement with PBC resulted in a reduction in fresh density, a phenomenon directly attributable to the substantial disparity in specific gravity between the constituent materials: PBC, with a specific gravity of approximately 1.69 g/cm³, compared to 3.15 g/cm³ for ordinary Portland cement.

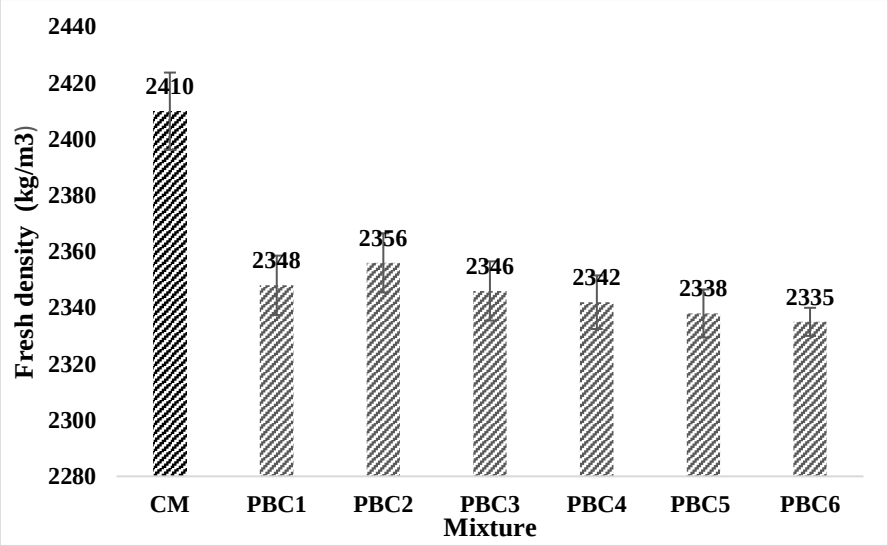

Figure 12. Fresh density mortar mixes

Fresh density measurements revealed that PBC5 and PBC6 exhibited reductions of 2.98% and 3.11%, respectively, compared to the control mix mortar. This progressive decrease in fresh density with increasing biochar content is consistent with findings reported in previous studies (Rupasinghe et al 2025). The reduction can be attributed to three primary mechanisms: (i) the highly porous microstructure of PBC, which sequesters mixing water within its internal pore network, thereby reducing the volume of free water available in the mixture; (ii) the high cation exchange capacity of biochar, which enhances physical bonding through hydrogen bonding interactions, further immobilizing water molecules; and (ii) The angular and irregular particle morphology of PBC can increase inter-particle friction and restrict fresh mortar mobility, particularly at higher replacement levels, as similar effects have been reported for biochar particles with porous surfaces and coarse morphology that adversely influence rheology, flowability, and workability of cementitious systems (Gupta & Kua 2019).

This geometric characteristic increases mechanical interlocking and inter-particle friction within the fresh mortar matrix. As biochar content increases, the cumulative effect of these angular particles progressively restricts the mobility and flow of the mixture, manifesting as reduced workability and lower packing efficiency, which in turn contributes to the observed density reduction.

3.3 Compressive strength

The compressive strength of PBC-modified mortar exhibited a dose-dependent response, with optimal performance observed at moderate replacement levels. As illustrated in **Figure 13**, the compressive strength development of the mortar mixes for 7 days and 28 days results demonstrate that biochar-modified specimens showed strength development over time, consistent with continued cement hydration.

At lower biochar dosages PBC 1-3 %, resulted in enhanced compressive strength relative to the control mortar. The optimal performance was achieved at 2 % and 3 % PBC, where at 7 days, the control mixture experienced a notable enhancement of 47.86 MPa in its compressive strength, advancing by roughly 22.54% from its initial strength measured at 7 days of curing to its strength recorded. This superior strength in the control mortar can be attributed to the unimpeded cement hydration process, which proceeds without interference from supplementary materials. Interestingly, PBC2 exhibited superior 7 days strength

compared to all the PBC suggesting an optimal biochar dosage exists. At the lower dosage PBC1, the quantity of biochar is insufficient to provide significant microstructural benefits such as pore refinement and enhanced nucleation sites for hydration products. Conversely, at the higher dosage PBC6, excessive biochar incorporation introduces detrimental effects including increased porosity, dilution of the cementitious binder, and the creation of weak interfacial zones between biochar particles and the cement matrix. The PBC2 formulation achieves an optimal balance, where the biochar content is sufficient to provide beneficial filler effects and nucleation sites without compromising the integrity of the cementitious matrix (Room et al 2025).

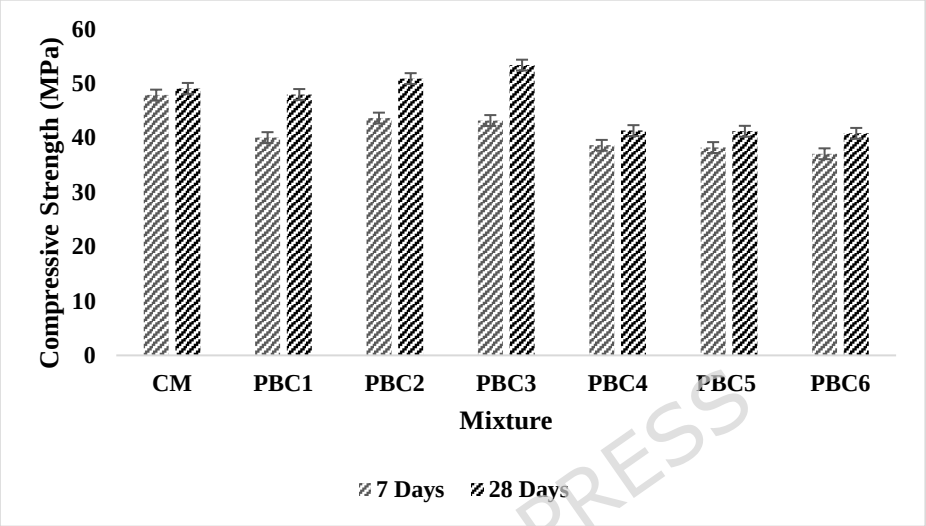

Figure 13. Compressive strength development of mortar mixes.

At 28 days of curing, the biochar-modified mortars PBC2 and PBC3 demonstrated superior compressive strength performance compared to the control specimen. Specifically, PBC3 achieved 52.37 MPa, while PBC2 attained 50.89 MPa (8.7%, 3.6%) improvement relative to the reference mortar. These strength enhancements align with findings reported by Zhao et al. (2024), who observed up to 13% compressive strength improvement at 28 days when plant-derived biochar was incorporated into cementitious materials. This strength enhancement can be attributed to the filler effect of fine biochar particles, which densify the cementitious matrix by filling capillary pores and improving the interfacial transition zone. However, at higher replacement levels, 4-6 %, a progressive decline in compressive strength was observed. Specifically, mortars containing 4%, 5%, and 6% PBC exhibited reductions in 28-day strength of 15.8%, 16% and 16.8%, respectively, relative to the control mix. The pronounced strength reduction observed at higher PBC dosages can be attributed to several interrelated mechanisms. Firstly, inadequate dispersion of biochar particles within the cementitious matrix leads to agglomeration and non-uniform distribution, creating weak zones that compromise structural integrity. Secondly, the highly porous microstructure of biochar particles absorbs mixing water, thereby reducing the water available for cement hydration in the surrounding matrix and consequently retarding early-age strength development. Thirdly, the porous nature of biochar introduces additional microstructural defects and voids, which act as stress concentrators and reduce the overall load-bearing capacity of the composite. Furthermore, the interfacial transition zone (ITZ) between biochar particles and the cement paste tends to be weaker due to poor bonding and increased porosity, further diminishing mechanical performance. These deleterious effects

have been consistently documented in previous investigations on biochar-modified cementitious materials (Yang et al 2021; Mosaberpanah et al 2024; Mahmoud et al 2025). This strength deterioration at elevated biochar contents is consistent with findings reported by Gupta et al (2021), who observed approximately 20% strength reduction when 8 wt% wood sawdust biochar was incorporated into cement mortar. The decline in strength at higher dosages can be attributed to the dilution effect, where excessive biochar replacement reduces the quantity of cementitious binder available for hydration, and the increased porosity introduced by the porous biochar particles aligns with the experimental findings.

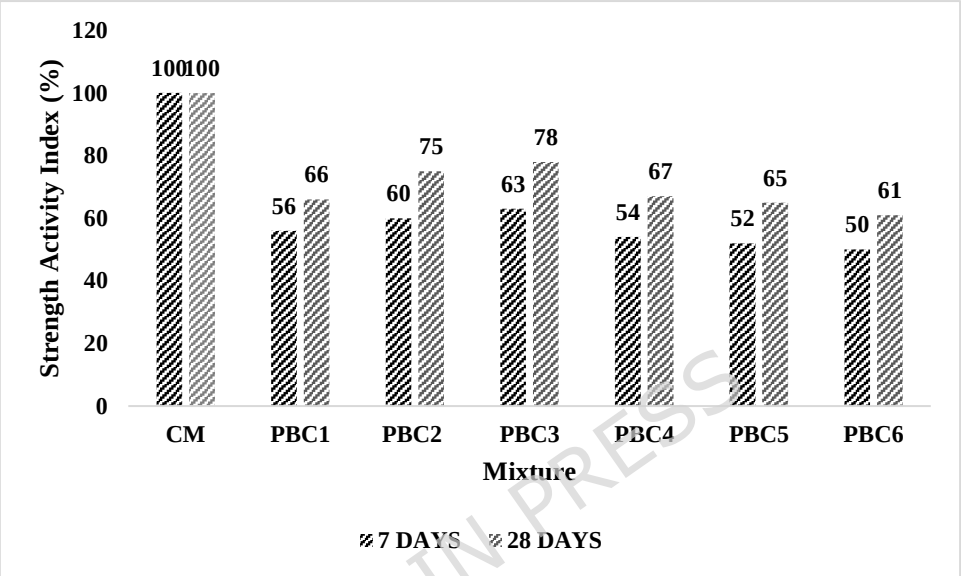

Figure 14. Strength Activity Index of the mortar mixes.

The strength activity index (SAI) values for all mixes at both 7 and 28 days, as presented in **Figure 14**, satisfy the minimum performance threshold of 75% specified in ASTM C618-19. Notably, the SAI values determined using the proposed constant volume methodology were comparable to those obtained through the conventional ASTM C311-18 procedure, which requires water content adjustment to achieve flow consistency per ASTM C618 requirements. This equivalence validates the efficacy of the constant volume approach as a viable alternative to the standard procedure. Relative to the control mortar, the formulation of the incorporation of PBC resulted in variable strength activity index values across different dosages. Formulations containing PBC5 and PBC6 exhibited slightly diminished SAI values, suggesting less favourable strength development relative to the reference mortar at 7 days (52 %, 50 %) and at 28 days (65%, 60%), showing marginally reduced SAI values, implying weaker strength progression in comparison to the control mixture. According to ASTM C618-19, a material must achieve a strength activity index (SAI) of at least 75% to be classified as a pozzolan. The SAI quantifies the pozzolanic reactivity of cement replacement materials by comparing the compressive strength of modified mixtures relative to a reference mortar. PBC2 and PBC3 formulations achieved SAI values of 75% and 78%, respectively, at 28 days, thereby satisfying the ASTM pozzolanic qualification criterion. The SAI results suggest that PBC may contribute to strength development through filler and possible secondary reaction effects; however, direct pozzolanic reactivity tests are required to confirm this behavior.

3.4 Flexural strength

The flexural strength development of PBC-modified mortar at 7 days and 28 days of curing at ambient temperature (20°C) is illustrated in **Figure 15.** At 7 days, all biochar-containing specimens exhibited reduced flexural strength relative to the control mixture, with strength reductions ranging from 2.01 MPa to 2.68 MPa, with a percentage reduction in strength of (13.2 % -34.9%). However, after 28 days of curing, a notable performance improvement was observed. The reference mortar achieved a flexural strength of. 3.22 MPa at 28 days, while the PBC2 and PBC3 respectively, surpassed this baseline value with an increase in strength of 3.44 MPa and 3.56 MPa. Notably, the PBC3 mixture demonstrated the highest flexural strength among all tested formulations, exceeding the control performance with a percentage increase in strength of 10.5% compared to the control mix. This enhancement can be attributed to several synergistic mechanisms, including the pozzolanic reactivity of the biochar, which contributes to the formation of additional cementitious products, and improved interfacial bonding between biochar particles and the cement matrix, which strengthens the composite microstructure and enhances resistance to bending stresses.

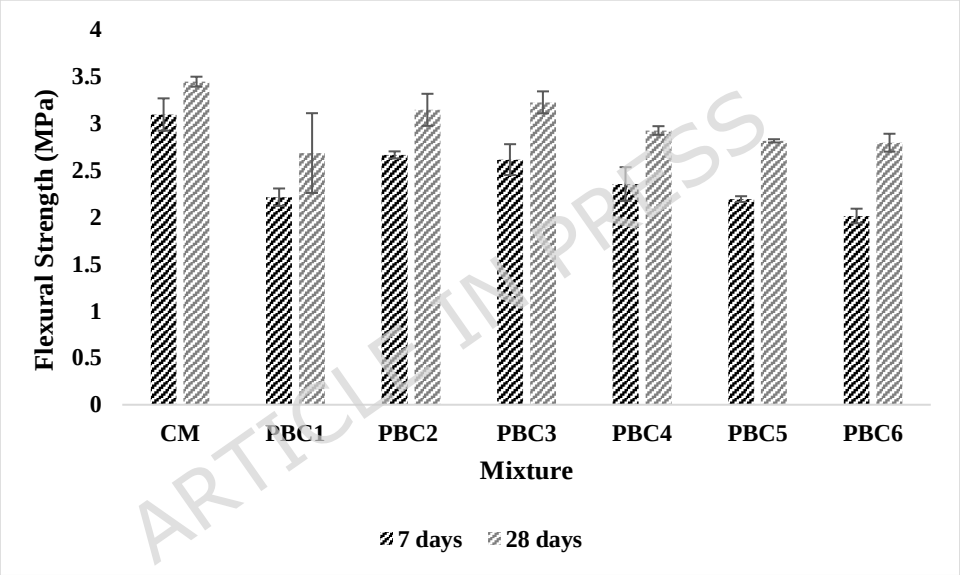

Figure 15. Flexural strength of mortar prisms.

Elevated biochar dosages introduce regions of high porosity within the cementitious matrix, which diminish the load-bearing cross-section available to resist tensile stresses. Consequently, these highly porous zones serve as preferential sites for crack nucleation and accelerate fracture propagation under loading. Ling et al (2023) demonstrated that excessive biochar content causes particle agglomeration due to van der Waals forces, resulting in the formation of larger pores and cracks that compromise the mechanical integrity of the composite. Similarly, Jedidi et al (2020) reported that while moderate incorporation of *Posidonia oceanica* fibres can improve specific mechanical properties, excessive fibre content compromises the interfacial adhesion between the reinforcement and the cement paste, leading to weakened composite performance.

Failure mechanisms of *Posidonia oceanicia* biochar cubes and prisms under loading

Post failure analysis of PBC specimens under uniaxial compression revealed three distinct failure modes influenced by biochar dosages seen in the **Figure 16**. Longitudinal splitting characterized by vertical cracks parallel to the loading direction predominated in optimal

dosage (PBC2- PBC3), indicating uniform m stress distribution and homogenous material behaviour. A conical fracture featuring an inclined shear plane from the loading surface was seen in PBC 4- PBC5, reflecting stress concentration and reduced bearing capacity due to increased porosity (Bagherzadeh, et al 2021). Lateral bulging is seen in PBC6, which represented a quasi–ductile failure mode with significant lateral deformation before ultimate failure, indicating that excessive biochar fundamentally alters mechanical response from brittle to ductile through an extensive void network and weak interfacial zones (Li et al 2024).

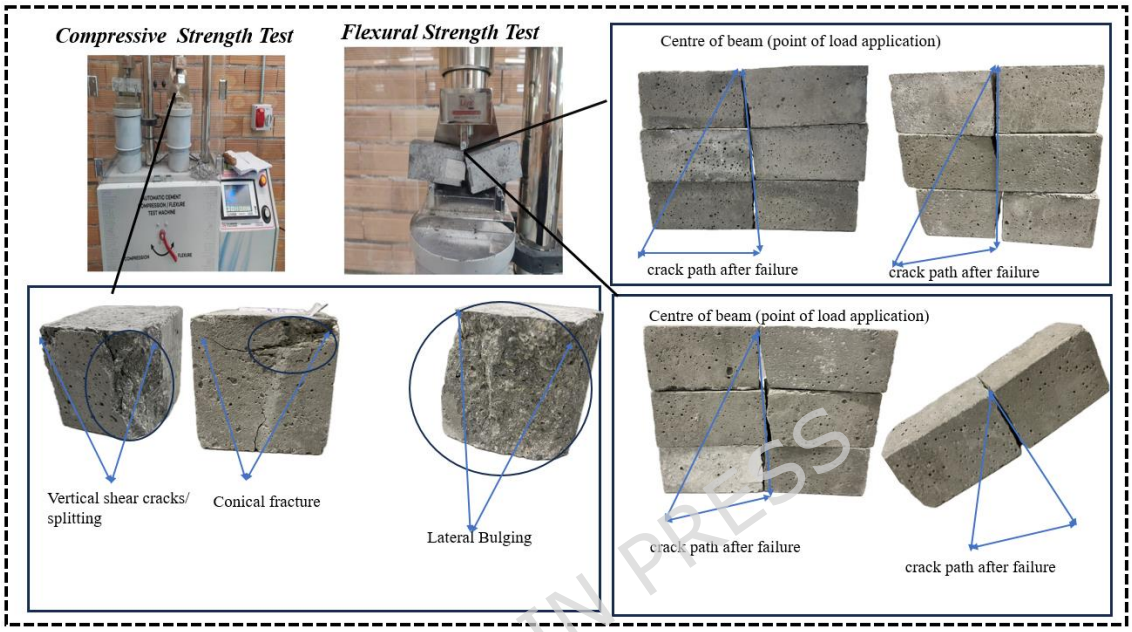

Figure 16. Failure modes observed during compression and flexural testing

Under three-point bending, PBC specimens exhibited vertical crack propagation from the tensile zone toward the compressive face seen in the Figure. While cracks generally aligned with the loading axis, the specimen with higher biochar content. Showed notable deviations, indicating non-uniform stress distribution caused by microstructural heterogeneity. The asymmetric cracking reveals that excessive biochar creates a preferential failure pathway, disrupting uniform stress transfer across the beam. A diagonal crack inclined at 20 °c was observed in specimens with an intermediate dosage of PBC 2-PBC3, indicating shear-dominated failure where combined bending shear stresses exceeded the material's tensile capacity near the support. This shear failure prior to full flexural capacity suggests that while optimal biochar dosages of PBC2 – PBC3 enhance compressive strength, they may create a weak interfacial zone susceptible to shear–induced separation, indicating the critical role of interfacial bond quality in controlling failure mechanism. Generally, the failure patterns of biochar cement composite are similar to that of concrete.

3.5 Hardened unit weight

The saturated surface dry (SSD) densities of the biochar-modified mortars, as illustrated in **Figure 17**, exhibited values ranging from 2330 kg/m³ to 2403 kg/m³ after 28 days of curing demonstrating a clear and consistent downward trend with increasing biochar replacement levels. The control mortar (CM) exhibited the highest density, approximately 2403 kg/m³. With each incremental addition of PBC, the density progressively decreased, reaching a minimum of approximately 2330 kg/m³ for the PBC6 mixture. This linear reduction in density is a direct and predictable consequence of replacing a portion of the dense cement binder

with a significantly lighter and more porous biochar material. The fundamental reason for the observed decrease in density is the substantial difference in the specific gravity of cement and PBC. Cement typically has a specific gravity of approximately 3.15. In contrast, biochar, being a lightweight, highly porous carbonaceous material, has a much lower specific gravity, often less than 1.8 and sometimes as low as 0.3 depending on the feedstock and pyrolysis conditions (Gupta et al 2018). By replacing a fraction of the heavier cement with an equivalent weight of lighter biochar, the overall mass of the composite per unit volume is inherently reduced. This finding is well-supported in the literature; for instance, Praneeth et al. (2021) reported that the density of mortars decreased by approximately 20% with a 40% biochar addition, highlighting the significant lightweight potential of biochar.

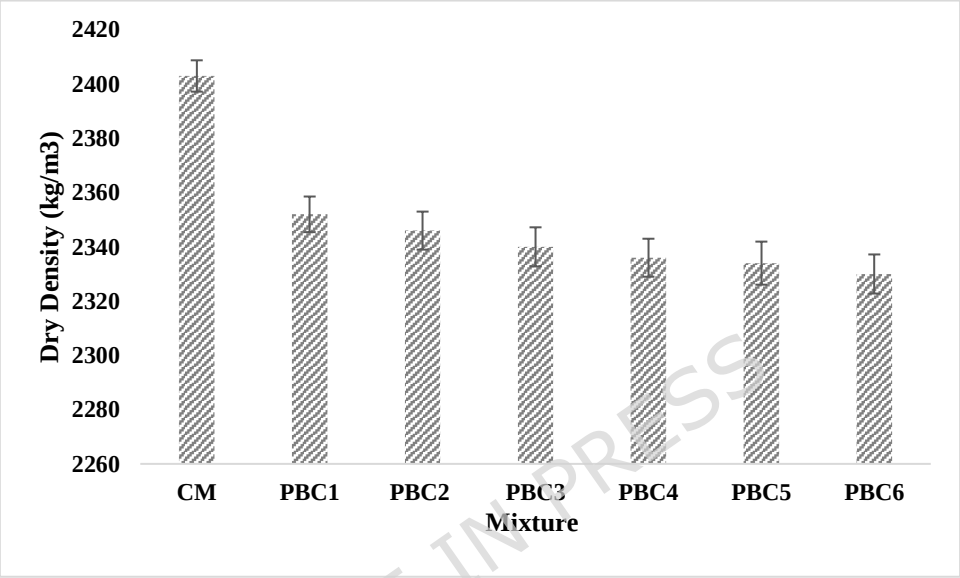

Figure 17. Dry density of hardened mortar mixes.

The reduction in density is also strongly correlated with the porosity results. As established, PBC dosages exceeding the optimal 2-3% level result in increased overall porosity due to particle agglomeration and the introduction of biochar's own internal pore network. Density and porosity are inversely proportional; an increase in the volume of voids (pores) within the matrix means a decrease in the volume of solid, dense material. Therefore, the higher porosity observed in the PBC4, PBC5, and PBC6 mixtures directly contributes to their lower measured dry densities. This inverse relationship between porosity and density is a well-established principle in materials science and has been consistently reported in studies on biochar-cement composites. The predictable reduction in density makes it a viable material for applications where reduced self-weight is desirable, such as in non-structural elements or lightweight precast panels. However, as noted in the mechanical strength analysis, this benefit must be carefully balanced against the concurrent reduction in compressive and flexural strength at higher dosages. The findings of Sirico et al. (2025) suggest that at optimal, low dosages 2 and 3%, the densification from the filler effect can counteract the lightweighting effect, resulting in no significant change in density. However, the data presented here clearly show that beyond this point, the lightweight effect caused by its low specific gravity and high porosity becomes the dominant factor.

3.6 Water absorption

It is widely recognized that materials with finer particle sizes demonstrate greater water absorption capacity due to their larger specific surface area. This increased surface area provides more sites for water molecule adsorption compared to materials composed of

coarser particles. **Figure 18** presents the water absorption mortar mixes containing varying proportions of cement composite (PBC), cured in water at 20°C for 28 days. The control mortar (CM) established a baseline water absorption of approximately 5.38%. A significant reduction in water absorption was observed at a low dosage, with the PBC1 mixture achieving the minimum value of 5.31%. Beyond this optimal point, water absorption progressively increased with rising biochar content. The PBC2 and PBC3 mixtures still showed improved performance compared to the control (5.34% and 5.36%), but by the PBC4 dosage, water absorption had surpassed the control and continued to climb, reaching a maximum value for the PBC6 mixture (6.35%, 6.97% and 7.5%). This trend indicates that while low concentrations of PBC are highly effective at enhancing the water tightness of the mortar, higher dosages are detrimental, leading to a more permeable and less durable matrix.

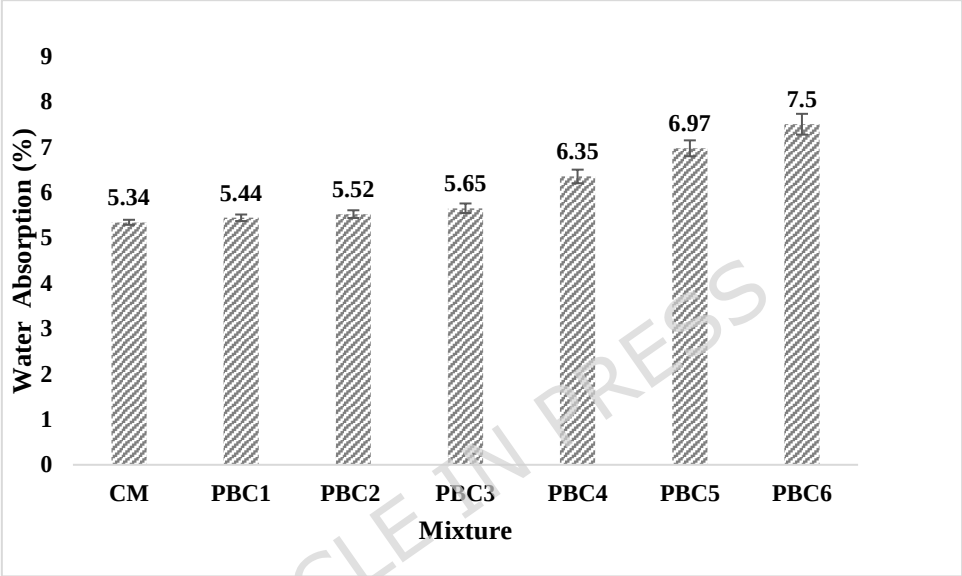

Figure 18. Water absorption of the mortar mixes.

The initial sharp decrease in water absorption, which is most pronounced in the PBC1 specimen, can be attributed to several complementary mechanisms that densify the cementitious matrix. Firstly, the fine biochar particles of 75 µm exert a physical filler effect, occupying the interstitial voids between cement grains. This leads to a more compact particle packing arrangement and a reduction in the volume of large, interconnected capillary pores, which are the primary pathways for water ingress (Gupta & Kua 2019).

The porous nature of PBC facilitates internal curing. The biochar absorbs a portion of the mixing water and gradually releases it back into the matrix as the cement hydrates. This process ensures a complete and more uniform hydration, leading to a refined pore structure with reduced connectivity (Mrad & Chehab 2019). However, the carbonaceous surfaces of the biochar particles act as nucleation sites, accelerating the precipitation of calcium-silicate-hydrate (C-S-H) gel. This accelerated formation of the primary binding phase further densifies the interfacial transition zone (ITZ) around the biochar particles and within the bulk paste, effectively blocking potential water pathways. Finally, the dispersion of these fine particles increases the tortuosity of the pore network, creating a more complex and convoluted path that significantly impedes the movement of water through the mortar.

3. 7 Porosity

The porosity hardened mortar mixes is depicted in **Figure 19,** exhibits a distinct and non-linear relationship with the biochar replacement level. The control mortar (CM) established a baseline porosity of approximately 11.56%. A marginal decrease in porosity was observed at low biochar dosages, with the PBC3 mixture achieving the lowest porosity of approximately 11.24%. Beyond this optimal point, the porosity demonstrated a consistent and significant increase with rising biochar content, reaching a maximum of approximately 14.96% for the PBC6. The initial reduction in porosity at 1% and 2% biochar content can be attributed to two primary physical mechanisms: the filler effect and improved particle packing. The fine biochar particles effectively fill the interstitial voids between cement grains, leading to a denser and more compact microstructure (Lorenzoni, et al 2024). This phenomenon is consistent with findings by Ye et al. (2025), who reported that porosity decreases at a biochar content of 1% 2. Furthermore, the biochar particles can serve as nucleation sites, promoting the precipitation of hydration products (C-S-H gel) and further densifying the matrix. This refined pore structure at low dosages is directly correlated with the enhanced mechanical performance observed in the compressive and flexural strength tests, where the PBC2 mixture demonstrated optimal strength.

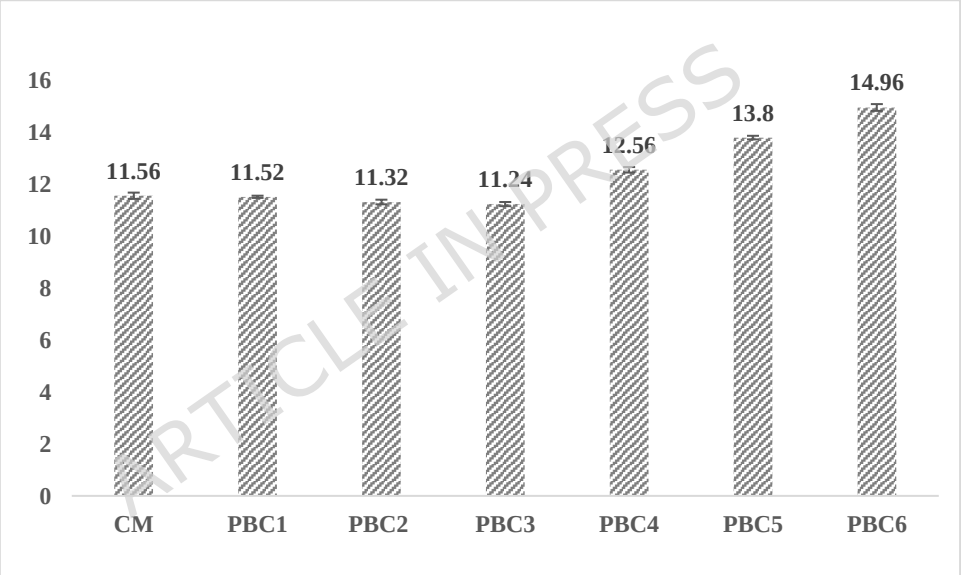

Figure 19. Porosity hardened mortar mixes.

The pronounced increase in porosity observed from 4% to 6% biochar content is a result of several overlapping detrimental effects. Firstly, at higher concentrations, biochar particles have a strong tendency to agglomerate due to van der Waals forces, creating large, poorly-bonded clusters (Barbhuiya et al 2024). These agglomerates introduce significant voids and prevent the formation of a continuous, homogeneous cement paste. This finding is strongly supported by Ling et al. (2023), who identified that excessive biochar content leads to agglomeration, resulting in the formation of more pores and cracks in the mortar. The inherently high internal porosity of PBC itself becomes a dominant factor. While beneficial for internal curing at low dosages, at higher replacement levels, there is insufficient cement paste to fill the extensive network of pores within the biochar particles, thereby increasing the overall void content of the composite. This aligns with the observations of Kushwah et al. (2024),

who noted that porosity in biochar-based mortar increases with dosage due to the rising total porosity within the cement

matrix. This increased porosity compromises the material's integrity by reducing the effective cross-sectional area available to resist mechanical loads, which explains the significant drop in compressive and flexural strength for the PBC5 and PBC6 mixtures.

3.8 Dry shrinkage

Cementitious composites are susceptible to autogenous shrinkage, a phenomenon resulting from the internal volume reduction that occurs as water is consumed from the capillary pore network during cement hydration. This volumetric contraction is governed by multiple interrelated factors, including the water-to-cement ratio, mixture proportions, curing regime, environmental conditions, heat of hydration, and ambient temperature (Wu et al 2017). The drying shrinkage of mortar specimens (25 × 25 × 285 mm) was evaluated in accordance with ASTM C596-18. All specimens were maintained in a controlled chamber at a temperature of 23 ± 2°C and a relative humidity of 50 ± 4% throughout the testing period. A beneficial reduction in shrinkage was observed at low dosages in **Figure 20** with the PBC3 mixture (3% biochar) exhibiting a remarkable 29.1% decrease in shrinkage compared to the control mortar (CM). However, beyond this optimal point, the trend reversed dramatically. The PBC4, PBC5, and PBC6 mixtures all demonstrated significantly higher shrinkage than the control, with the PBC6 specimen showing a 44.0% increase. This behavior indicates that while low concentrations of biochar are highly effective at mitigating shrinkage, higher dosages are detrimental and exacerbate it. The significant reduction in drying shrinkage at low biochar dosages, particularly at the 3% replacement level, is primarily attributed to the internal curing effect provided by the porous biochar particles (Senadheera et al 2023). During mixing, the biochar absorbs a substantial amount of water and then gradually releases it back into the cementitious matrix as the internal relative humidity drops due to cement hydration and drying. This slow release of water replenishes the moisture consumed in the hydration process and lost to the environment, which effectively mitigates both autogenous and drying shrinkage by reducing the development of capillary stresses. The increase in drying shrinkage at dosages of 4% - 6% can be explained by two dominant negative factors. Firstly, the high-water absorption capacity of biochar becomes an adverse effect. Secondly, at higher concentrations of PBC, the material's extensive internal porosity functions as a water reservoir, sequestering substantial quantities of moisture within its interconnected pore network. During the drying phase, the progressive evaporation of water from these biochar-hosted pores generates pronounced capillary tension and internal tensile stresses within the cementitious matrix. This moisture depletion mechanism amplifies the magnitude of shrinkage strain, as the loss of pore water creates localized stress concentrations that exceed the matrix's tensile capacity, ultimately resulting in enhanced volumetric contraction.

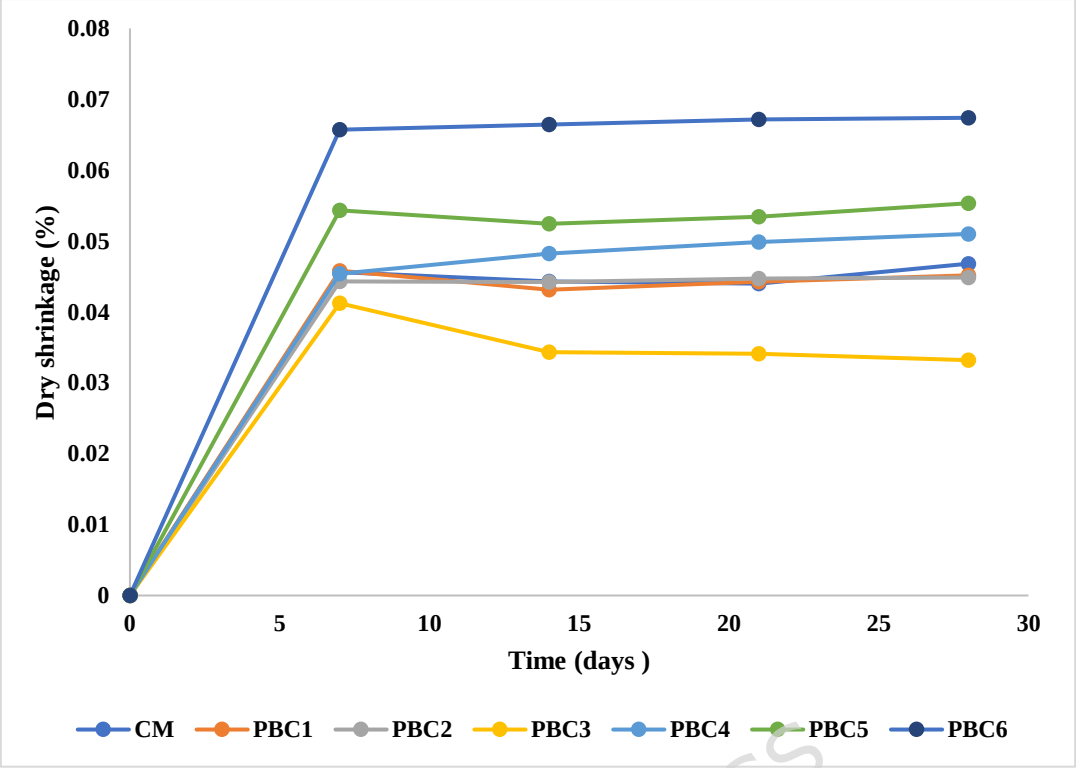

Figure 20. Dry shrinkage of the mortar mixes.

3.10 Acid attack resistance

Evaluating the durability of the biochar-modified mortars (PBC) incorporation as a partial cement replacement on the acid resistance of mortars is essential for enhancing the durability of cementitious composites subjected to aggressive acidic environments. **Figure 21** presents residual compressive strength of the mixtures after sulfuric acid exposure. The performance of all mixtures following a 28-day immersion in a 5% sulfuric acid solution, with mass loss and residual compressive strength serving as the primary indicators of degradation. The deterioration mechanism involves the reaction between sulfuric acid and calcium hydroxide (portlandite) present in the hydrated cement paste, forming expansive and soluble calcium compounds such as gypsum ($CaSO_4 \cdot 2H_2O$). The formation and subsequent crystallization of these reaction products within the pore structure generate internal tensile stresses, leading to microcracking, spalling, and progressive loss of both mass and mechanical strength in the mortar specimens. The control mortar (CM) exhibited the poorest performance among all tested formulations after 28 days of immersion in a 5% sulfuric acid solution, with the compressive strength declining to 35.07 MPa and the cumulative mass loss reaching 7.2%. In contrast, the biochar-modified mortars demonstrated substantially enhanced acid resistance. The PBC3 specimen, which had the highest initial strength (52.37 MPa), also retained the highest absolute strength after acid exposure, ending with 41.49 MPa. This corresponds to a strength loss of only 21.4%, far superior to the control. Similarly, the PBC1 and PBC2 mixtures lost only 18.5% and 20.2% of their strength, respectively. This demonstrates that the same mechanisms that contribute to high initial strength at optimal dosages also impart excellent chemical resistance. The mixtures with higher PBC content (PBC4, PBC5, and PBC6), despite having lower initial strengths, showed a greater relative resistance to acid attack than the control. For instance, PBC4 lost only

12.9% of its strength. This consistent trend across all dosages indicates that biochar provides an inherent protective quality to the cementitious matrix. As established in the porosity and water absorption analyses, the addition of biochar at low dosages (1-3%) acts as a physical filler and promotes a more complete hydration process through internal curing. This creates a denser, less permeable microstructure with a more tortuous and disconnected pore network. This refined pore structure physically hinders the ingress of the aggressive sulfate and hydrogen ions from the acid solution, slowing down the rate of degradation. A less permeable matrix means that the acid has limited access to the vulnerable cement paste within the core of the specimen (Tee et al 2023).

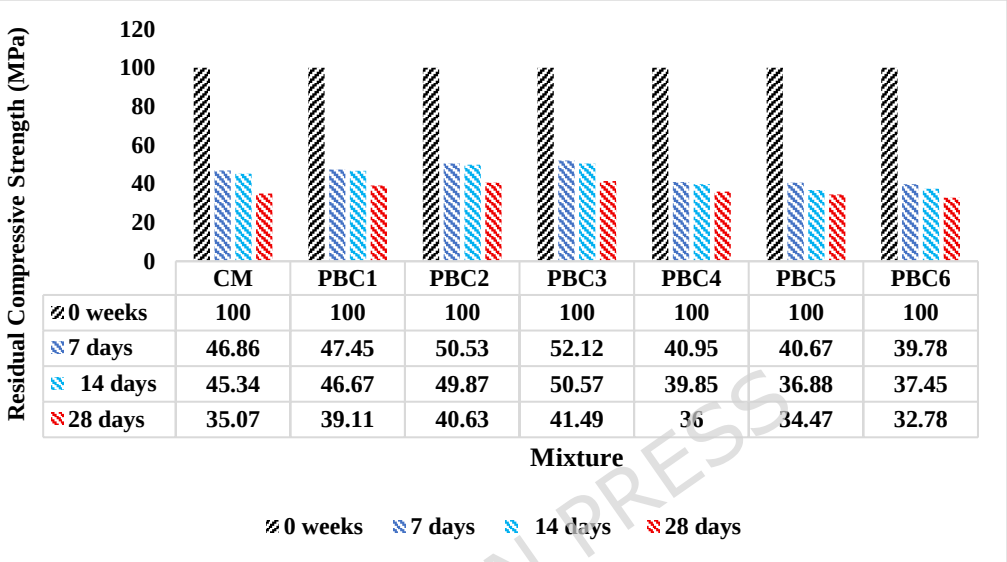

	CM	PBC1	PBC2	PBC3	PBC4	PBC5	PBC6
0 weeks	100	100	100	100	100	100	100
7 days	46.86	47.45	50.53	52.12	40.95	40.67	39.78
14 days	45.34	46.67	49.87	50.57	39.85	36.88	37.45
28 days	35.07	39.11	40.63	41.49	36	34.47	32.78

Figure 21. Residual compressive strength of the mixtures after sulfuric acid exposure.

The primary targets of calcium hydroxide (portlandite) are the most soluble and vulnerable components of hydrated cement paste. Through its pozzolanic activity, PBC consumes a portion of this $Ca(OH)_2$ to form additional, more durable C-S-H gel. By reducing the amount of this primary target, biochar makes the matrix chemically more stable and less susceptible to acid degradation. This explains that the post-acid strength for the PBC mixes is proportionally higher relative to their initial strength compared to the control. PBC itself is a carbonaceous and chemically stable material, far more resistant to acid than the alkaline cement paste. The dispersed biochar particles act as inert micro-scale barriers, disrupting the continuous path of acid penetration and shielding the surrounding C-S-H gel from direct attack. This contributes to the entire resilience of the composite material. These findings are well-aligned with previous research. Studies by Sikora et al. (2022) and Singh et al. (2025) have consistently shown that incorporating biochar improves the acid resistance of cementitious composites. The combination of a denser microstructure and a more chemically robust matrix makes the biochar-modified mortars, particularly those with 1-3% biochar, significantly more durable and suitable for application in aggressive acidic environments.

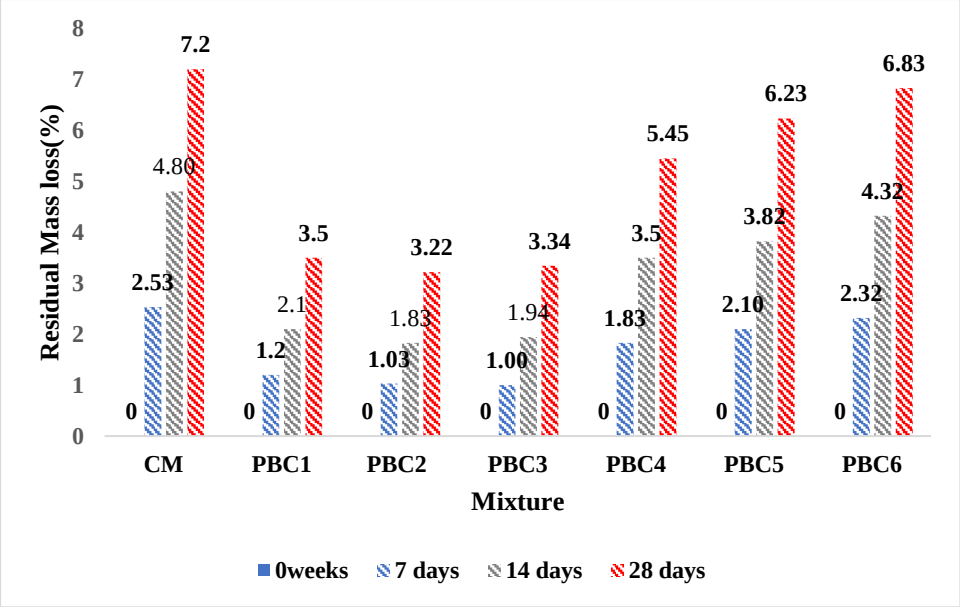

Figure 22. Residual Mass loss of the mixtures after sulfuric acid exposure.

Figure 22 presents the residual mass loss of the mixtures after sulfuric acid exposure. The progressive mass loss of all mortar specimens over the 28-day immersion period in a 5% sulfuric acid solution. This clearly illustrates that mass loss increases over time for all mixtures, which is expected during continuous acid exposure. However, the rate and extent of this degradation vary significantly depending on the biochar content, showing the profound impact of PBC on the durability of the mortar. The control mortar (CM) consistently demonstrated the poorest performance, as indicated by the highest final mass loss value of approximately 7.2% at 28 days. This represents the baseline degradation of conventional mortar, where the acid attack leads to the dissolution of cement hydration products and the formation of expansive salts like gypsum, resulting in significant material erosion and spalling. The superior performance of the PBC3 mixtures can be attributed to two primary mechanisms. Firstly, the pore refinement caused by the filler effect of fine biochar particles creates a denser, less permeable microstructure. This physically hinders the ingress of the aggressive acid solution, protecting the vulnerable cement paste in the core of the specimen. Secondly, the pozzolanic activity of biochar consumes a portion of the highly susceptible calcium hydroxide ($Ca(OH)_2$) to form more durable C-S-H gel, reducing the amount of material that can be easily attacked and leached by the acid (Aneja et al 2022). The biochar content increases beyond the optimal of PBC4, PBC5, and PBC6, the mass loss also increases, although it remains lower than that of the control mortar. This trend suggests that at higher dosages, the negative effects of increased porosity and potential particle agglomeration begin to counteract the protective benefits. The higher porosity in these mixes provides more pathways for acid ingress compared to the dense matrix of PBC1, PBC2 and PBC3. Nevertheless, the fact that even PBC6 of 6.8% mass loss performed better than the control mix of 7.2% mass loss indicates that the inherent chemical stability and barrier effect of biochar still provide a net protective benefit.

A visual inspection of the mortar specimens presented in **Figure 23** shows the surface degradation mass loss and colour changes after sulfuric acid attack after 28 days of sulfuric acid immersion provides a compelling physical confirmation of the degradation trends observed in the mass loss and residual compressive strength data. The control mortar (CM) specimen exhibited the most severe deterioration. The surface was

characterized by significant erosion and spalling, with a distinct whitish layer of gypsum deposits clearly visible. This appearance is indicative of a classic acid attack mechanism, the acid solution readily penetrated the relatively porous matrix and reacted with the abundant calcium hydroxide ($Ca(OH)_2$), forming expansive and weak secondary products that destroyed the structural integrity of the cement paste from the outside in. An interesting observation in the PBC1, PBC 2 and PBC3 specimens was the development of minor surface expansion, serves as visual evidence of their effective resistance to acid ingress. This swelling represents a defensive response where the dense microstructure trapped the expansive reaction products near the surface, preventing them from propagating inward and causing internal damage. The low water absorption rates measured for these mixtures provide the mechanistic explanation; their refined pore networks effectively blocked the pathways that would otherwise allow acid to infiltrate the bulk material.

The specimens PBC4, PBC5, and PBC6 excessive biochar content dilutes the cement paste and disrupts the formation of calcium-silicate-hydrate (C-S-H) gel, the primary binding phase responsible for strength development. This results in a weaker, more porous matrix that is inherently more susceptible to sulfuric acid attack. During acid exposure, the calcium hydroxide and residual calcium-bearing phases react with sulfuric acid to form calcium sulfate (gypsum), which precipitates within the enlarged pore spaces. Interestingly, while the control and optimal biochar specimens experienced net mass loss due to the dissolution and leaching of reaction products, the high-biochar specimens exhibited a different behavior. The relatively large and open pore structure of these mixtures provided sufficient space for gypsum crystals to accumulate without being readily washed away, leading to a net mass loss in some cases. This phenomenon was similarly reported by Mosaberpanah et al (2023), who observed mass gain in specimens with 3% biochar content after acid exposure. However, it is critical to note that this mass gain does not indicate improved performance; rather, it reflects the accumulation of weak, expansive secondary products within a compromised matrix, which ultimately contributes to reduced compressive strength and structural integrity.

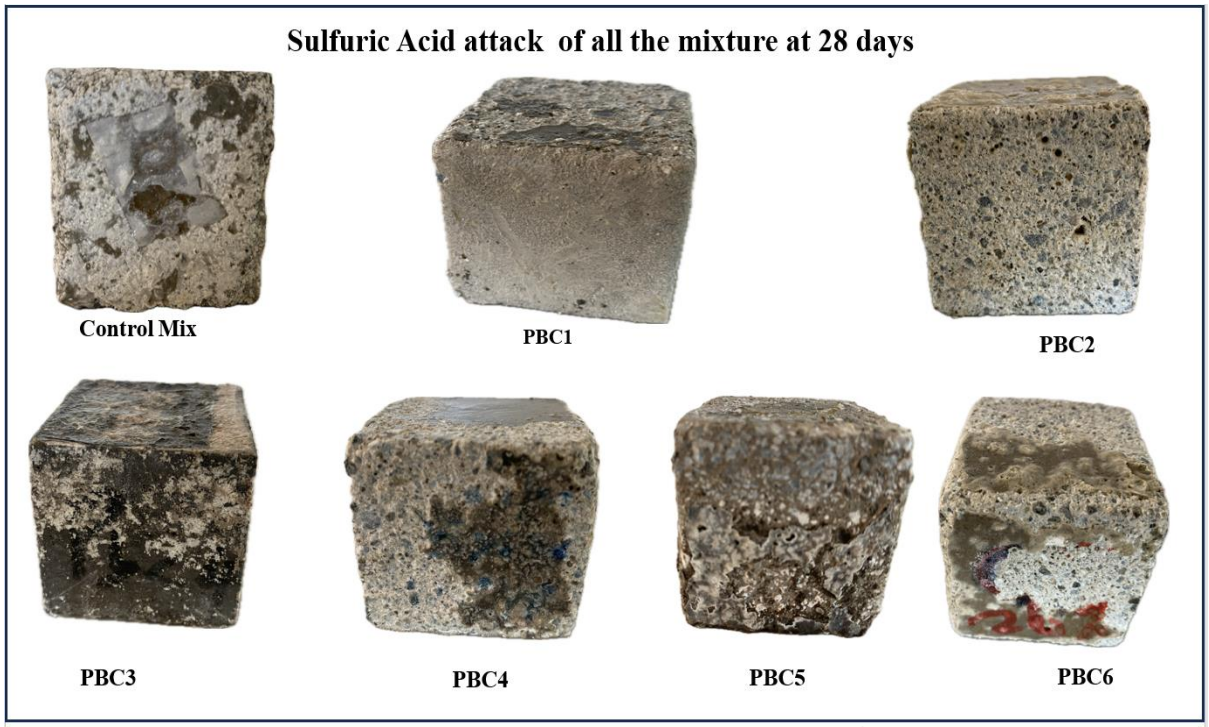

Figure 23. Surface degradation showing mass loss and colour changes after sulfuric acid attack

3.11 High-temperature resistance

The incorporation of PBC in cementitious mortar can influence the hydration kinetics and the microstructural development of the hardened matrix. When cement-based materials are subjected to elevated temperatures, they undergo a series of thermally-induced changes that progressively degrade their physical and mechanical properties. To establish a consistent baseline for thermal testing and to isolate the effects of elevated temperature exposure from those of residual moisture, all specimens were pre-dried in an oven at 105°C for 24 hours before thermal testing. This procedure removes free water while preserving the integrity of the hydrated cement phases. Previous research has demonstrated that significant microcracking in concrete typically becomes evident only at temperatures exceeding 200°C [95], as the thermal expansion mismatch between aggregate and paste, combined with the onset of C-S-H dehydration, generates internal tensile stresses that exceed the matrix's capacity. The high-temperature resistance of the biochar-modified mortar formulations was systematically evaluated. **Figure 24** presents the residual strength loss in the mixtures. The control mix and biochar-modified mortars after exposure to elevated temperatures of 200°C, 400°C, and 600°C. The results reveal a complex but clear relationship between PBC content, exposure temperature, and thermal stability. At 200°C, cementitious materials typically experience an initial phase of degradation primarily due to the evaporation of free and physically adsorbed water from the capillary pores. As shown, the control mortar (CM) exhibited a compressive strength of approximately 40.32 MPa after exposure to 200°C. Notably, all the biochar-modified mixtures, from PBC1 to PBC6, demonstrated superior or comparable strength at this temperature. The optimal mixtures, PBC2 and PBC3, achieved the highest strengths of 48.39 MPa and 51.36 MPa, respectively. This initial

advantage is likely attributable to the denser and more refined microstructure of these mortars at ambient conditions, a result of the filler effect and enhanced hydration from biochar's pozzolanic activity, which provides a more robust starting point against thermal degradation.

Exposure to 400°C shows a critical threshold where more severe degradation mechanisms are initiated. At this temperature, the chemically bound water within the calcium-silicate-hydrate (C-S-H) gel begins to dehydrate, and the decomposition of calcium hydroxide ($Ca(OH)_2$) commences. These processes lead to significant microstructural damage and a substantial loss of strength in conventional mortars. The control mortar's strength dropped to 38.03 MPa, showing a clear decline. However, the protective effect of biochar becomes highly evident at this stage. The PBC2 and PBC3 mixtures maintained their strength exceptionally well, at 48.66 MPa and 51.03 MPa, respectively, showing minimal loss compared to their 200°C values. This superior performance is primarily attributed to the vapor pressure release mechanism (Yang et al 2021). The interconnected pore network within the biochar particles provides escape pathways for the water vapour generated within the matrix. By dissipating this internal pressure, the biochar prevents the formation of destructive tensile stresses that would otherwise cause explosive spalling and severe microcracking.

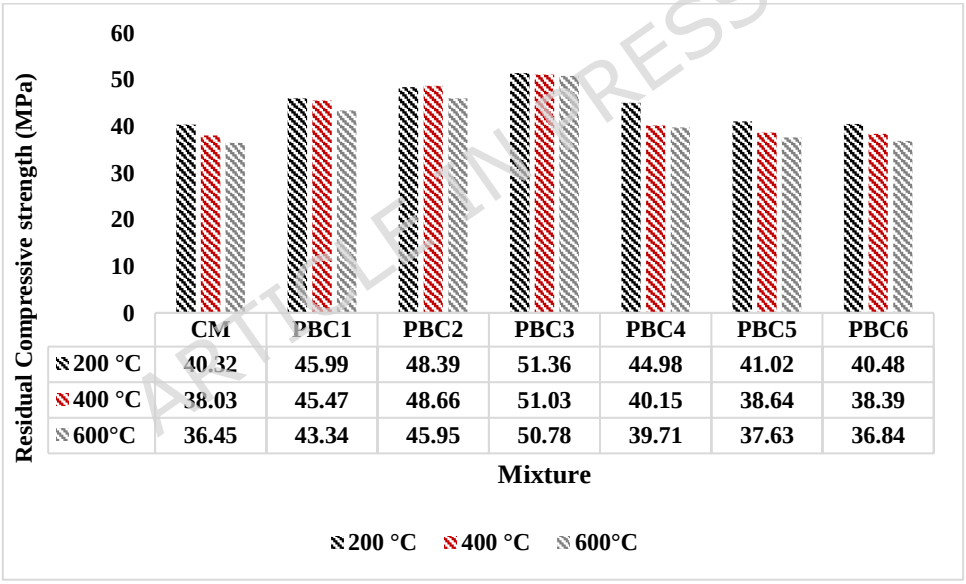

Figure 24. Residual strength loss in the mixtures

At 600°C, cementitious material faces critical damage, characterized by the complete dissolution of $Ca(OH)_2$ and severe degradation of C-S-H binder, leading to a drastic loss of structural integrity. The control mortar reached its lowest strength of 36.45 MPa, a significant reduction from its initial state. In remarkable contrast, the PBC3 specimen retained a compressive strength of 50.78 MPa, demonstrating virtually no strength loss between 200°C and 600°C. This exceptional thermal stability shows that the protective effects of biochar are most pronounced at higher, more critical temperatures. Additionally, the dispersed biochar particles function as crack deflection sites, impeding the propagation of thermally-generated micro fractures through energy dissipation mechanisms, thereby maintaining matrix integrity. These observations corroborate the findings of Wang et al. (2024), who demonstrated enhanced high-temperature performance in cementitious systems with 1-2% biochar incorporation. The biochar formulations of PBC4, PBC5 and PBC6 exhibited a performance decline attributable

to competing microstructural effects. Although the vapour pressure mitigation and crack deflection mechanisms remained active, the substantial reduction in C-S-H gel volume and concomitant increase in matrix porosity diminished the intrinsic thermal resistance of these specimens. Consequently, while these mixtures outperformed the control mortar, their residual strengths were markedly inferior to those of the optimal PBC2 and PBC3 formulations (Mensah et al 2021). **Figure 25** presents the thermal effect on the mortar at different temperatures. The mortar specimens after being exposed to various temperatures of 200°C, 400°C and 600°C. At this initial stage of thermal exposure, the primary physical process is the evaporation of free and loosely bound water from the capillary pores. The visual evidence confirms that no severe structural damage, such as major cracking or explosive spalling, has occurred in any of the mixtures. However, subtle differences in surface appearance and colour are apparent, providing preliminary insights into the material's thermal response. The most notable observation was a slight colour change to a lighter, beige hue in the optimal biochar mixtures PBC1, PBC2 and PBC3, indicating an initial thermal interaction. The mixtures PBC4 and PBC6 remained darker, with PBC5 showing minor surface roughness.

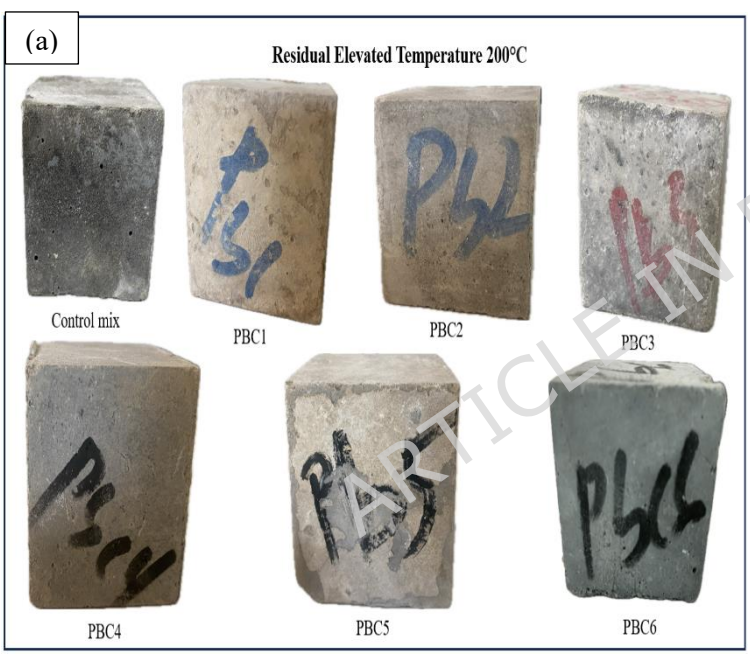

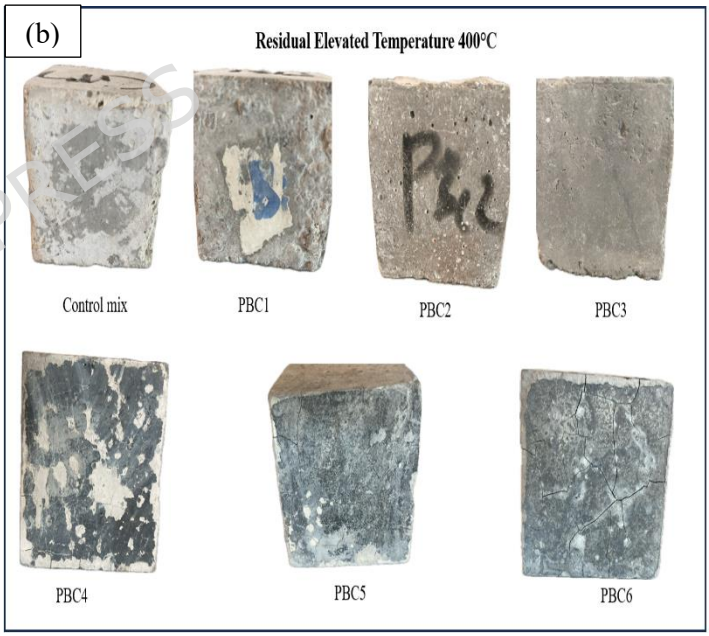

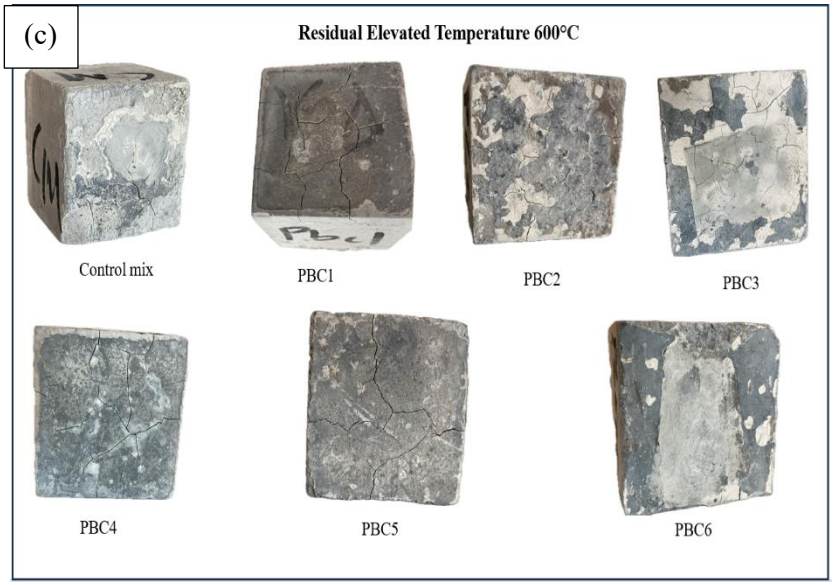

Figure 25. Thermal Effect on the Mortar at Different Temperatures (a) Residue Elevated Temperature at 200°C (b) Residue Elevated Temperature at 400°C (c) Residue Elevated Temperature at 600°C

At 400°C, the onset of severe thermal degradation was seen. At this stage, the dehydration of C-S-H gel and the initial decomposition of calcium hydroxide ($Ca(OH)_2$) generate significant internal stresses. The visual evidence clearly differentiates the performance of the mixtures, revealing a dramatic divergence in thermal stability that was not apparent at 200°C. the performance of the mixtures dramatically diverged. The control mortar (CM) and PBC1 showed considerable surface degradation and corner spalling. In contrast, the PBC3 specimen remained remarkably intact, with sharp edges and no visible cracks, visually demonstrating the effectiveness of the vapour pressure release mechanism. The mixtures PBC4 -PBC6 began to exhibit catastrophic failure. PBC4 and PBC5 suffered from severe surface spalling, while PBC6 displayed extensive map-cracking, a clear sign of internal stress overwhelming the weak, porous matrix.

At 600°C, a temperature associated with severe thermal conditions and the complete decomposition of key binder components, the performance differences reached their zenith. The control mortars, PBC4, PBC5 and PBC6 experienced catastrophic failure, characterized by deep, interconnected cracks, fragmentation, and a complete loss of cohesion. Conversely, the PBC2 and PBC3 specimens, in an extraordinary display of thermal resilience, remained structurally intact.

3.12 Microstructural analysis

The micrographs, presented in **Figure 26** reveal a distinct evolution in the matrix morphology and integrity corresponding to the biochar dosage. The microstructure of the blended cement mixture demonstrated a significantly improved interfacial transition zone (ITZ) between the cement paste and aggregate. The matrix appears dense and well-compacted, characterized by a continuous Calcium-Silicate-Hydrate (C-S-H) gel, which is the primary binding phase responsible for the material's strength. The identifiable, angular grains and needle-like ettringite crystals formed during the hydration process. The porosity is relatively low, consisting mainly of small, disconnected capillary pores. This dense and homogeneous microstructure is typical

of a standard Portland cement mortar and serves as a benchmark for evaluating the effects of biochar addition. The microstructures of the PBC2 and PBC3 specimens, respectively, the biochar appears to be well-integrated into the cementitious matrix. The PBC2 specimen reveals a dense matrix surrounding the aggregate, with a refined pore structure compared to the control. PBC3 shows the well-developed Interfacial Transition Zone (ITZ) between the biochar/aggregate and the cement paste. The particles also exhibit angular shapes with variable sizes, which may influence packing density and workability. Additionally, some micro-cracks and voids are visible on the PBC surface; while these may reduce mechanical interlocking, they could also serve as active sites for chemical interaction with the cementitious phases. The presence of a stable carbonaceous matrix observed in the SEM images further suggests good thermal resistance, supporting the improved residual strength of PBC-containing composites at elevated temperatures. The observation aligns with recent studies, which have found that biochar can act as a nucleation site, promoting the formation of additional hydration products (Zhao et al 2024). Ling et al. (2023) demonstrated that an optimal biochar dosage of 1-3% facilitates a secondary reaction where $Ca(OH)_2$ is consumed to form additional, strength-enhancing C-S-H gel, effectively filling pores and densifying the matrix. Furthermore, research by Zhu et al. (2023) has shown that a Ca-rich layer of hydration products can form at the biochar-paste interface, creating a strong chemical and mechanical bond. This enhanced ITZ and densified matrix in PBC2 and PBC3 directly explain their superior mechanical performance and thermal resilience.

The excessive PBC6 has introduced significant defects that compromise the material's integrity. Large macro-pores and voids are prevalent throughout the matrix, creating a discontinuous and weakened structure. The ITZ in the PBC6 specimen is notably weak and poorly defined, with clear evidence of interfacial cracks between the biochar particles and the cement paste. This indicates poor bonding and creates pre-existing pathways for failure. This finding is consistent with the work of Lorenzoni et al. (2024), who concluded that high volume fractions of biochar can act as flaws within the microstructure, leading to a reduction in mechanical properties. The high-water absorption of excessive biochar also locally de-waters the cement paste, hindering proper hydration and leading to a porous, friable matrix. This compromised and defect-ridden microstructure is directly responsible for the significantly lower compressive strength of PBC6 and its catastrophic failure under thermal loading.

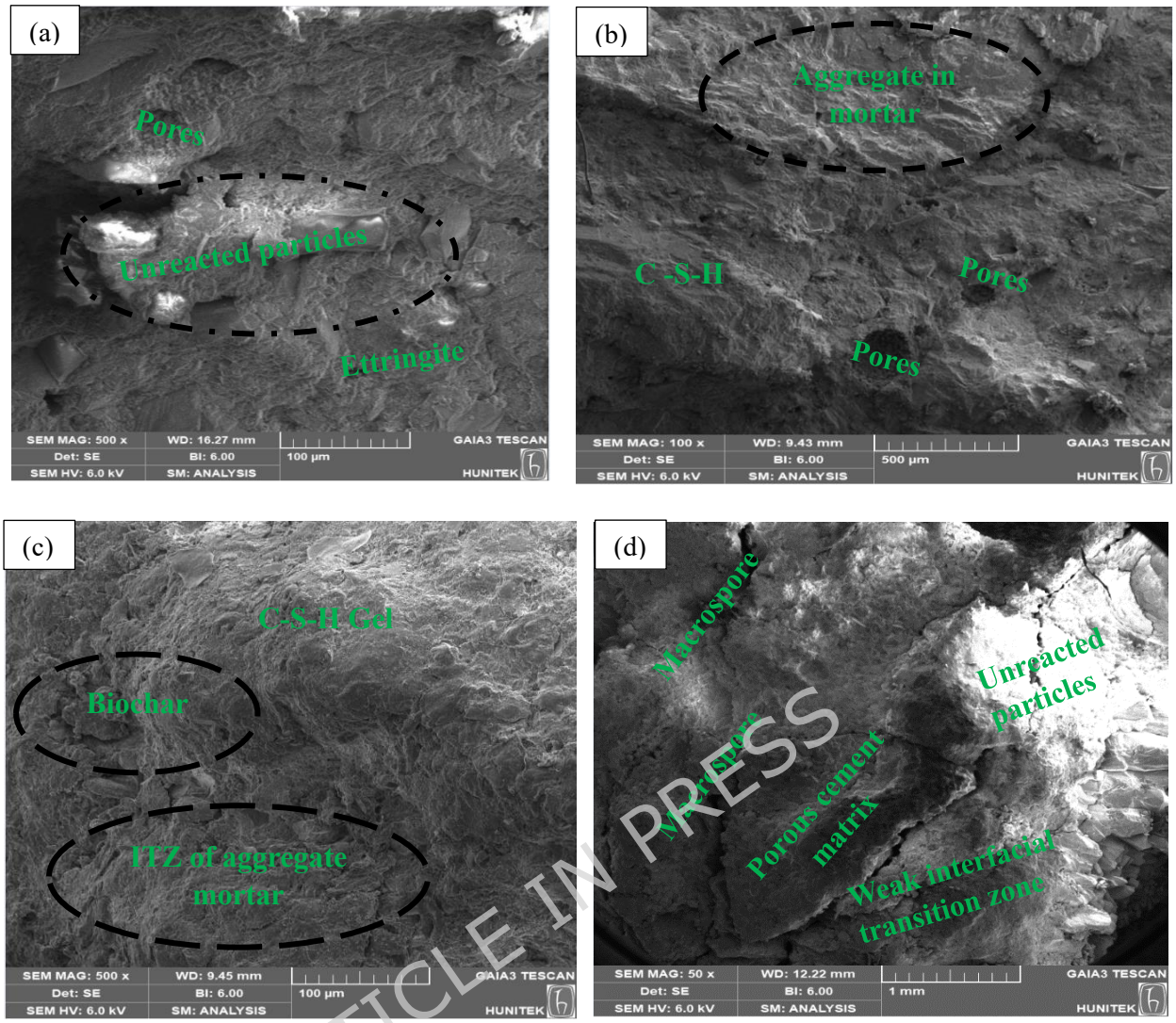

Figure 26. SEM image of (A) Control mix ITZ of cement, microcrack and pores (B) PBC2 Dense interfacial zone with C–S–H gel and pores **(**C) PBC3 Dense Interfacial Transition Zone (D) SEM PBC6 Macropores, weak interfacial transition zone, Unreacted particles

3.13 Fourier Transform Infrared Spectroscopy (FTIR)

The Fourier-transform infrared (FTIR) spectra of the control mix and PBC modified blends (1%, 2%, 3%, 5%, and 6%) shown in **Figure 27** demonstrate noticeable alterations in the vibrational bands of key functional groups, indicating chemical and microstructural interactions resulting from PBC content. The broad band observed between 3600–3200 cm^{-1} corresponds to O–H stretching vibrations, which are associated with bound water and hydroxyl groups in hydration products such as C–S–H gel. The presence of this band in all mixtures confirms ongoing hydration. A slight variation in intensity with increasing PBC content suggests modifications in moisture retention and internal curing effects attributed to the porous structure of PBC. The band at 1650–1600 cm^{-1} is assigned to H–O–H bending vibrations, indicating physically adsorbed water within the matrix. The relatively consistent intensity across the mixes implies that PBC incorporation does not hinder the hydration process but may influence water distribution within the microstructure. The absorption peak around 1450–1410 cm^{-1} corresponds to C–O stretching vibrations, typically associated with carbonate formation ($CaCO_3$). According to Haris Javed et al. (2022), the inclusion of biochar accelerates

carbonation and contributes to microstructural refinement by obstructing pores and microcracks, which eventually improves durability and limits fluid penetration. The presence of this band suggests slight carbonation, which is common in cementitious systems exposed to atmospheric CO_2. The strong band observed between 1100–1000 cm^{-1} represents Si–O–Si stretching vibrations, primarily attributed to the silicate network of C–S–H gel, which is the principal hydration product responsible for enhancing the mechanical strength and durability of the mortar (Jo et al., 2017). Changes in peak intensity and slight shifts among PB mixes indicate alterations in the silicate structure, suggesting that PBC may influence the polymerization degree of hydration products. The peak at 950–900 cm^{-1} is linked to Si–O stretching vibrations of C–S–H, confirming the formation of primary hydration products. Enhanced intensity in some PBC-modified mixes may indicate improved hydration or microstructural refinement. The consistent presence of this band across all samples confirms structural stability of the cementitious matrix.

Overall, the FTIR results demonstrate that incorporating PBC does not introduce detrimental chemical phases but slightly modifies the intensity of key hydration-related bands. This suggests that PBC primarily influences the microstructure and hydration kinetics rather than altering the fundamental chemical composition of the cement matrix.

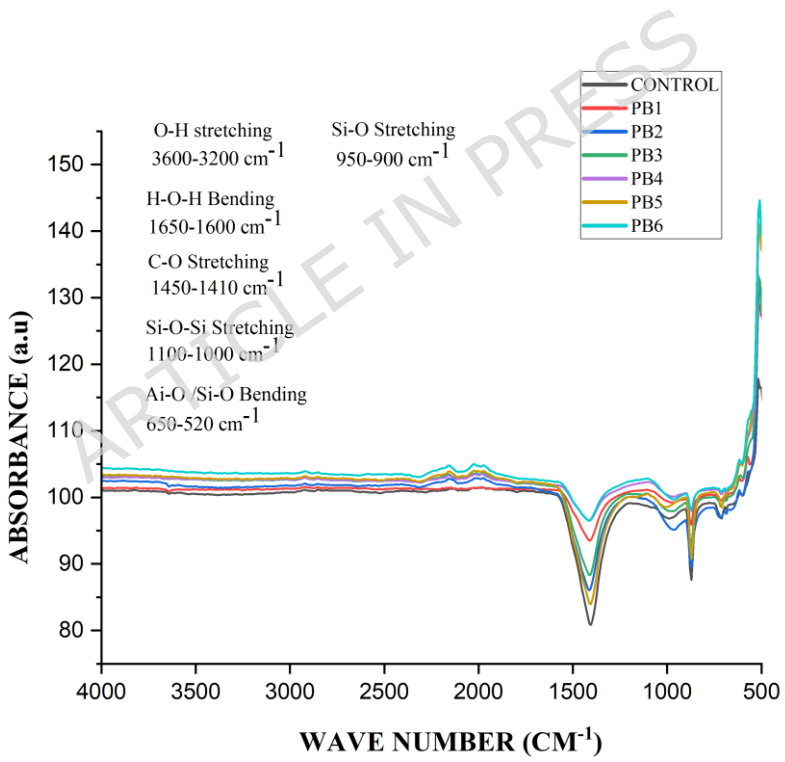

Figure 27: FTIR of the mortar mixes.

4. Sustainability Assessment

The sustainability assessment of the various biochar–modified mortar mixes is presented in the **Figure 28**. Total embodied carbon decreased progressively from the control mix to PBC6 of 831 $kgCO_2/kg$ to 786 $kgCO_2/kg$, representing a maximum reduction of 5.3%. However, eco-strength efficiency defined as the ratio of compressive strength to embodied

carbon peaked at PBC3 (0.065), indicating an optimal balance between mechanical performance and environmental sustainability. Beyond PBC3 biochar replacement, the decline in compressive strength outpaced the carbon reduction benefits, resulting in diminished eco- efficiency. Therefore, PBC3 represents the most sustainable formulation, achieving 2.53% carbon reduction while maintaining superior strength to carbon performance. The reduction in embodied carbon observed with PBC incorporation is comparable to reductions reported for other low-carbon cement strategies, including supplementary cementitious materials, alternative binders, and engineered composite modifications, which typically achieve carbon savings ranging from approximately 5% to 40% depending on replacement level and material processing conditions (Scrivener et al., 2018; Habert et al., 2020; Hamed et al., 2024). This comparison indicates that PBC performs competitively among emerging sustainable cement technologies while additionally contributing to marine biomass waste valorization.

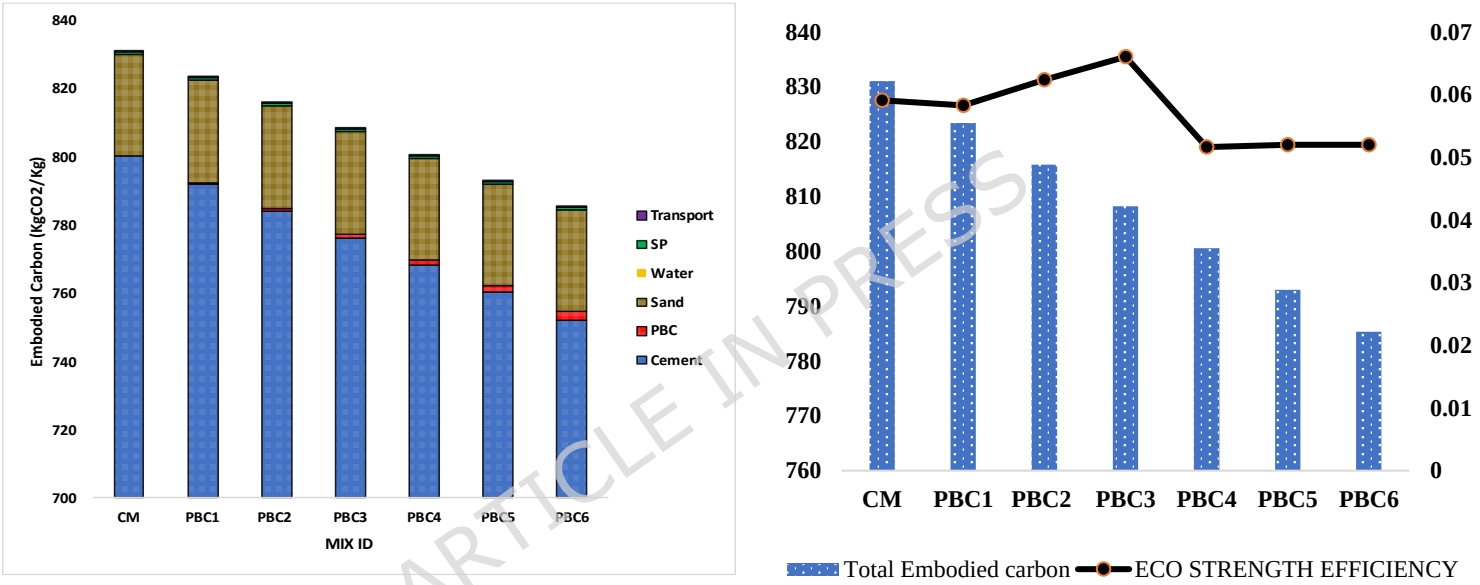

Figure 28. Total embodied carbon and strength efficiency of biochar-modified composites compared to control mortar

5. Statistical significance using one-way ANOVA

In this study, a one-way Analysis of Variance (ANOVA) was conducted to quantify the effect of mix composition (CM, PBC1- PBC6) on the fresh, mechanical, and durability properties of PBC-modified mortar. The experimental program was conducted at a 95% confidence level ($\alpha = 0.05$) using triplicate measurements for each mix. The test was applied to assess whether the differences among the means were statistically significant. This approach enabled a statistical assessment of whether variations in PBC content significantly influenced the measured properties. The F-statistic was used to compare the variance between group means with the variance within groups. A large F-value accompanied by a p-value less than 0.05 indicates that the differences among the mixes are statistically significant and not due to random experimental variation. The ANOVA results demonstrated that mix composition had a statistically significant effect on all evaluated properties, as summarized in **Table 6.**

Table 6: Analysis of variance (ANOVA) summary for properties of PBC-modified mortar

Experimental test	Df (Between, Within)	F-Value	p-Value	R^2	Significance
Flow	6,14	6.62	0.00176	0.739	Significant
Density	6,14	39.02	<0.0001	0.944	Significant
CS_{7days}	6,14	19.26	<0.0001	0.892	Significant
CS_{28days}	6,14	114.48	<0.0001	0.980	Significant
WA	6,14	1118.31	<0.0001	0.998	Significant

The ANOVA results indicate that PBC dosage had a statistically significant effect on all evaluated properties. The flowability analysis yielded $F(6,14) = 6.62$, $p = 0.00176$, indicating that changes in PBC content significantly influenced workability. The coefficient of determination ($R^2 = 0.739$) shows that approximately 73.9% of the variation in flow is explained by mix composition. Density was significantly affected by PBC incorporation, with $F(6, 14) = 39.02$ and $p < 0.0001$. The high R^2 value of 0.944 indicates that 94.4% of the variability in density is attributable to changes in PBC dosage. The compressive strength at 7 days, the ANOVA produced $F(6,14) = 19.26$ ($p < 0.0001$), confirming a statistically significant influence of PBC on early-age strength development ($R^2 = 0.892$). At 28 days, the effect was even more pronounced, with $F(6,14) = 114.48$ and $p < 0.0001$. The very high R^2 value of 0.980 demonstrates an excellent model fit, indicating that long-term strength is strongly governed by mix composition. Water absorption exhibited the highest statistical sensitivity to PBC content, with $F(6,14) = 1118.31$ and $p < 0.0001$. The near-unity R^2 value (0.998) confirms that PBC dosage almost entirely explains the variation in water absorption. However, all the p-values were below 0.05, the null hypothesis of equal group means was rejected for all response variables. These findings confirm that PBC content significantly influences the mechanical and durability performance of the mortar.

6. Concluding remarks

This study investigated the performance of mortar incorporating PBC as a partial cement replacement. The results demonstrate that PBC influences fresh, mechanical, thermal, microstructural, and environmental properties in a dosage-dependent manner.

1. Flowability decreased with increasing PBC content due to the porous structure and irregular morphology of the particles, although mixtures containing up to 3% replacement maintained acceptable workability.
2. Mechanical performance improved at low replacement levels (1–3%), with the 3% mixture exhibiting the highest compressive strength, exceeding the control mix by 8.7%. This enhancement is attributed primarily to particle packing effects and matrix densification. Higher replacement levels (4–6%) resulted in strength reductions associated with increased porosity and weaker interfacial bonding.

3. Thermal resistance strength retention, with the 3% mixture maintaining structural integrity after exposure to 600 °C, whereas higher dosages showed structural deterioration.
4. Microstructural observations confirmed these findings, revealing refined pore structure at low PBC contents and whereas high doses generated macro-voids, interfacial cracks, and discontinuities that served as failure initiation sites.
5. Environmental assessment showed progressive reductions in embodied carbon with increasing biochar content, reaching a maximum reduction of 5.3% at 6% replacement; higher biochar reduces carbon yet weakens strength, limiting sustainability gains. however, the optimal balance between mechanical performance and sustainability occurred at 3%.
6. The one-way ANOVA results confirm that PBC dosage has a statistically significant influence on all evaluated fresh, mechanical, and durability properties of the mortar ($p < 0.05$). The consistently high F-values and large coefficients of determination ($R^2 = 0.739–0.998$) indicate that mix composition is the dominant factor governing performance variation.
7. FTIR results indicate that PBC incorporation alters the chemical structure of the cement matrix, reflecting interactions with hydration products and modifications in microstructural development.

Overall, the results indicate that low-dosage incorporation of PBC can enhance mortar performance while reducing environmental impact, demonstrating its potential as a sustainable supplementary material in cementitious system.

Limitation and future scope

The current study offers significant novel knowledge about the fresh, hardened, and durability characteristics of mortar production that contains PBC. Despite the comprehensive experimental program conducted, several limitations should be acknowledged. First, the study evaluated short-term mechanical, durability, and thermal properties; long-term performance, such as creep, shrinkage, carbonation resistance, and chloride penetration were not investigated. Second, although strength activity index results were obtained, direct pozzolanic reactivity tests were not performed, limiting definitive interpretation of the chemical contribution of PBC. Third, only a limited replacement range (1–6%) was examined; wider dosage ranges may further clarify threshold behaviour and performance limits. In addition, the experimental program was conducted under controlled laboratory conditions, which may not fully represent field performance.

Future research should focus on optimizing biochar properties, including pore structure, composition, and morphology, to enhance cementitious performance. Improved control of pyrolysis conditions and long-term monitoring are required to ensure structural reliability. Durability should be evaluated under aggressive environments such as sulfate, chloride, carbonation, freeze–thaw, and marine exposure. Verification of chemical reactivity is also needed through standardized pozzolanic tests (e.g., Chapelle and Frattini) supported by advanced analyses such as TGA/DTG to quantify hydration products. In addition, validation at the concrete scale is necessary to confirm practical applicability. These efforts will provide the scientific basis for large-scale implementation of biochar in sustainable cement-based materials.

Author Contributions: Stephen Babajide Olabimtan: conceptual framework, assessment, methodological approach, materials, writing preliminary draft, and

modification of writing. Mohammad Ali Mosberpanah: conceptual framework, assessment, methodological approach, materials, writing preliminary draft, and modification of writing. Babatunde olufunso Oluwole: conceptual framework, assessment, methodological approach, materials, writing preliminary draft, and modification of writing. All authors have read and agreed to the published version of the manuscript.

Funding: This research received no external funding.

Institutional Review Board Statement: Not applicable.

Informed Consent Statement: Not applicable.

Data Availability Statement: Data will be made available upon request.

Conflicts of Interest: The authors declare no conflict of interest.

REFERENCES

1. Akinyemi, B. A., & Adesina, A. (2020). Recent advancements in the use of biochar for cementitious applications: A review. *Journal of Building Engineering*, *32*, 101705. doi: https://doi.org/10.1016/j.jobe.2020.101705.
2. Ali, A. Y. F., Ahmed, S. A., & El-Feky, M. S. (2025). Alkali-activated concrete with expanded polystyrene: A lightweight, high-strength solution for fire resistance and explosive protection. *Journal of Building Engineering*, *99*, 111648. https://doi.org/10.1016/j.jobe.2024.111648
3. Aneja, A., Sharma, R. L., & Singh, H. (2022). Mechanical and durability properties of biochar concrete. *Materials Today: Proceedings*, *65*, 3724-3730.
4. ASTM C138/C138M-17a, 2017, "Standard Test Method for Density (Unit Weight), Yield, and Air Content (Gravimetric) of Concrete," ASTM International, West Conshohocken, PA, ASTM
5. ASTM C1437-20; Standard Test Method for Flow of Hydraulic Cement Mortar. ASTM International: West Conshohocken, PA, USA, 2020.
6. ASTM C267-20; Standard Test Methods for Chemical Resistance of Mortars, Grouts, and Monolithic Surfacing's and Polymer Concretes. ASTM International: West Conshohocken, PA, USA, 2020,www.astm.org.
7. ASTM C305-20; Standard Practice for Mechanical Mixing of Hydraulic Cement Pastes and Mortar of Plastic Consistency. ASTM International: West Conshohocken, PA, USA, 2020
8. ASTM C311/C311M-18; Historical Standard: Standard Test Methods for Sampling and Testing Fly Ash or Natural Pozzolans for Use in Portland-Cement Concrete. ASTM International: West Conshohocken, PA, USA, 2018
9. ASTM C348-21 (2021). "Standard Test Method for Flexural Strength of Hydraulic-Cement Mortars". ASTM International, West Conshohocken, PA, 2021, www.astm.org.
10. ASTM C596-18; Standard Test Method for Drying Shrinkage of Mortar Containing Hydraulic Cement. ASTM International: West Conshohocken, PA, USA, 2018.
11. ASTM C642-13. (2013). "Standard Test Method for Density, Absorption, and Voids in Hardened Concrete". ASTM International, West Conshohocken, PA, 2013, www.astm.org.
12. ASTM C642-13; Standard Test Method for Density, Absorption, and Voids in Hardened Concrete. ASTM International: West Conshohocken, PA, USA, 2021, www.astm.org.

13. ASTM E119-20; Standard Test Methods for Fire Tests of Building Construction and Materials. ASTM International: West Conshohocken, PA, USA, 2020, www.astm.org.
14. ASTMC109-21; Standard Test Method for Compressive Strength of Hydraulic Cement Mortars (Using 2-in. or [50 mm] Cube Specimens). ASTM International: West Conshohocken, PA, USA, 2021
15. ATEŞ, A. Investigation of physicochemical and chemical properties of biochar activated with carbonate, nitrate, and borohydride. *Biomass Conv. Bioref.* **15**, 2397–2407 (2025). https://doi.org/10.1007/s13399-024-05323-9
16. Babajide Olabimtan, S., & Mosaberpanah, M. A. (2023). The implementation of a binary blend of waste glass powder and coal bottom ash as a partial cement replacement toward more sustainable mortar production. *Sustainability*, *15*(11), 8776.
17. Bagherzadeh, P., Goshtasbi, K., Kazemzadeh, E., Kashef, M., & Aloki Bakhtiari, H. (2021). Stress-dependence of the permeability, porosity, and compressibility in fractured porous media regarding fracturing condition. *Bulletin of Engineering Geology and the Environment*, *80*(6), 5091-5110.
18. Barbhuiya, S., Das, B. B., & Kanavaris, F. (2024). Biochar-concrete: A comprehensive review of properties, production and sustainability. Case Studies in Construction Materials, 20, e02859. https://doi.org/10.1016/j.cscm.2024.e02859
19. Bărbulescu, A., & Hosen, K. (2025). Cement industry pollution and its impact on the environment and population health: a review. *Toxics*, *13*(7), 587.
20. Ben Hadj Tahar D, Triki Z, Guendouz M, Tahraoui H, Zamouche M, Kebir M, Zhang J, Amrane A. Characterization and thermal evaluation of a novel bio-based natural insulation material from Posidonia oceanica waste: a sustainable solution for building insulation in Algeria. ChemEngineering. 2024 Feb 2;8(1):18. doi.org/10.3390/chemengineering8010018.
21. Chaturvedi, K., Singhwane, A., Dhangar, M., Mili, M., Gorhae, N., Naik, A., ... & Verma, S. (2024). Bamboo for producing charcoal and biochar for versatile applications. *Biomass Conversion and Biorefinery*, *14*(14), 15159-15185.
22. Chen, W., Yang, S., Zhang, X., Jordan, N. D., & Huang, J. (2022). Embodied energy and carbon emissions of building materials in China. *Building and environment*, *207*, 108434. /doi.org/10.1016/j.buildenv.2021.108434
23. Cocozza, C.; Parente, A.; Zaccone, C.; Mininni, C.; Santamaria, P.; Miano, T. Comparative management of offshore posidonia residues: Composting vs. energy recovery. *Waste Manag.* 2011, *31*, 78–84.
24. Danish, A., Mosaberpanah, M. A., Salim, M. U., Fediuk, R., Rashid, M. F., & Waqas, R. M. (2021). Reusing marble and granite dust as cement replacement in cementitious composites: A review on sustainability benefits and critical challenges. *Journal of Building Engineering*, *44*, 102600.
25. El-Feky, M. S., & El-Rayes, M. (2019). The effect of nano cellulose synthesized from rice straw on the performance of cement composite reinforced with carbon nano tubes. *Int. J. Sci. Technol. Res*, *8*(10), 2401-2410.
26. Gunasekaran, P. K., & Chin, S. C. (2024). Performance of bamboo biochar as partial cement replacement in mortar. *Materials Today: Proceedings*, *109*, 53-61.
27. Gupta, S., & Kashani, A. (2021). Utilization of biochar from unwashed peanut shell in cementitious building materials–Effect on early age properties and environmental benefits. *Fuel Processing Technology*, *218*, 106841. https://doi.org/10.1016/j.fuproc.2021.106841
28. Gupta, S., & Kua, H. W. (2019). Carbonaceous micro-filler for cement: Effect of particle size and dosage of biochar on fresh and hardened properties of cement mortar. *Science of the Total Environment*, *662*, 952-962.

29. Gupta, S., & Kua, H. W. (2019). Carbonaceous micro-filler for cement: Effect of particle size and dosage of biochar on fresh and hardened properties of cement mortar. *Science of the Total Environment*, *662*, 952-962.
30. Gupta, S., Kua, H. W., & Dai Pang, S. (2018). Healing cement mortar by immobilization of bacteria in biochar: An integrated approach of self-healing and carbon sequestration. *Cement and Concrete Composites*, *86*, 238-254.
31. Gupta, S., Kua, H. W., & Low, C. Y. (2018). Use of biochar as carbon sequestering additive in cement mortar. *Cement and concrete composites*, *87*, 110-129. https://doi.org/10.1016/j.cemconcomp.2017.12.009
32. Gupta, S., Muthukrishnan, S., & Kua, H. W. (2021). Comparing influence of inert biochar and silica rich biochar on cement mortar–Hydration kinetics and durability under chloride and sulfate environment. *Construction and Building Materials*, *268*, 121142. https://doi.org/10.1016/j.conbuildmat.2020.121142
33. Hamdaoui O, Ibos L, Mazioud A, Safi M, Limam O. Thermophysical characterization of Posidonia Oceanica marine fibers intended to be used as an insulation material in Mediterranean buildings. Construction and building materials. 2018 Aug 20; 180:68-76. doi.org/10.1016/j.conbuildmat.2018.05.195
34. Hamed, N., Serag, M. I., El-Attar, M. M., & El-Feky, M. S. (2024). High early strength concrete incorporating waste derived nanomaterials for sustainable construction. *Scientific Reports*, *14*(1), 30602.
35. Hammond, G. P., & Jones, C. I. (2008). Embodied energy and carbon in construction materials. *Proceedings of the institution of civil engineers-energy*, *161*(2), 87-98.
36. Javed, M. H., Sikandar, M. A., Ahmad, W., Bashir, M. T., Alrowais, R., & Wadud, M. B. (2022). Effect of various biochars on physical, mechanical, and microstructural characteristics of cement pastes and mortars. *Journal of Building Engineering*, *57*, 104850.
37. Javed, M. H., Sikandar, M. A., Ahmad, W., Bashir, M. T., Alrowais, R., & Wadud, M. B. (2022). Effect of various biochars on physical, mechanical, and microstructural characteristics of cement pastes and mortars. *Journal of Building Engineering*, *57*, 104850.
38. Jedidi M, Abroug A. Valorization of Posidonia oceanica Balls for the Manufacture of an Insulating and Ecological Material. Jordan Journal of Civil Engineering. 2020 Jul 1;14(3).
39. Jo, B. W., Sikandar, M. A., Chakraborty, S., & Baloch, Z. (2017). Strength and Durability Assessment of Portland Cement Mortars Formulated from Hydrogen-Rich Water. *Advances in Materials Science and Engineering*, *2017*(1), 2526130.
40. Kavindi, G. A. G., Tang, L., & Sasaki, Y. (2025). Assessing GHG emission reduction in biomass-derived biochar production via slow pyrolysis: A cradle-to-gate LCA approach. *Resources, Conservation and Recycling*, *212*, 107900.
41. Keiluweit, M., Nico, P. S., Johnson, M. G., & Kleber, M. (2010). Dynamic molecular structure of plant biomass-derived black carbon (biochar). *Environmental science & technology*, *44*(4), 1247-1253.
42. Khadir FK, Adebanjo AU, Shafiq N, Farhan SA, Adeosun JO. Assessing Photocatalytic Degradation in High-Performance Concrete Mixes Using Fourier Transform Infrared Analysis and Response Surface Modelling.
43. Khoury, G. A. (2000). Effect of fire on concrete and concrete structures. *Progress in structural engineering and materials*, *2*(4), 429-447. https://doi.org/10.1002/pse.51
44. Kumar, A., Bhattacharya, T., Shaikh, W. A., Chakraborty, S., Sarkar, D., & Biswas, J. K. (2022). Biochar modification methods for augmenting sorption of

contaminants. *Current Pollution Reports*, *8*(4), 519-555. doi: https://doi.org/10.1007/s40726-022-00238-3

45. Kuqo A, Boci I, Vito S, Vishkulli S. Mechanical properties of lightweight concrete composed with Posidonia oceanica fibres. Zastita Materijala. 2018 Dec 15;59(4):519-23. doi.org/10.5937/zasmat1804519k
46. Kushwah, S., Singh, S., Agarwal, R., Nighot, N. S., Kumar, R., Athar, H., & Naik B, S. (2024). Mixture of biochar as a green additive in cement-based materials for carbon dioxide sequestration. *Journal of Materials Science: Materials in Engineering*, *19*(1), 27.
47. Li, M., Zhu, X., Zhang, Y., & Tsang, D. C. (2024). A multi-phase mechanical model of biochar–cement composites at the mesoscale. *Computer-Aided Civil and Infrastructure Engineering*, *39*(23), 3552-3572.
48. Ling, Y., Wu, X., Tan, K., & Zou, Z. (2023). Effect of Biochar Dosage and Fineness on the Mechanical Properties and Durability of Concrete. Materials, 16(7), 2809. https://doi.org/10.3390/ma16072809
49. Liu, Z., Jiao, Y., Zhang, Y., Li, P., & Du, Y. (2025). Partial replacement of silica fume with waste glass powder in UHPC: Filling micropores and promoting hydration. *Construction and Building Materials*, *490*, 142581.
50. Lorenzoni, R., Cunningham, P., Fritsch, T. *et al.* Microstructure analysis of cement-biochar composites. *Mater Struct* **57**, 175 (2024). https://doi.org/10.1617/s11527-024-02452-5
51. Mahmoud, A. A., El-Sayed, A. A., Fathy, I. N., Fawzy, S., Alturki, M., Elfakharany, M. E., ... & Nabil, I. M. (2025). Evaluation of rice husk biochar influence as a partial cement replacement material on the physical, mechanical, microstructural, and radiation shielding properties of ordinary concrete. *Scientific Reports*, *15*(1), 27229. https://doi.org/10.1038/s41598-025-11987-8
52. Makepa, D. C., & Chihobo, C. H. (2025). Sustainable pathways for biomass production and utilization in carbon capture and storage a review. *Biomass Conversion and Biorefinery*, *15*(8), 11397-11419.
53. Malekzadeh, M., & Bilsel, H. (2014). Use of posidonia oceanica ash in stabilization of expansive soils. *Marine Georesources & Geotechnology*, *32*(2), 179-186.
54. Mensah, R. A., Shanmugam, V., Narayanan, S., Razavi, N., Ulfberg, A., Blanksvärd, T., ... & Das, O. (2021). Biochar-added cementitious materials—a review on mechanical, thermal, and environmental properties. *Sustainability*, *13*(16), 9336.
55. Mohammadi Ghahsareh, F., Guo, P., Jaha, N., Bao, Y., Khayat, K. H., & Meng, W. (2026). Advances and Challenges in Nano-modified Cementitious Composites: Mechanisms, Dispersion Strategies, and Impact on Mechanical Properties.
56. Mosaberpanah, M. A., Olabimtan, S. B., Balkis, A. P., Rabiu, B. O., Oluwole, B. O., & Ajuonuma, C. S. (2024). Effect of biochar and sewage sludge ash as partial replacement for cement in cementitious composites: mechanical, and durability properties. *Sustainability*, *16*(4), 1522.
57. Mrad, R., & Chehab, G. (2019). Mechanical and microstructure properties of biochar-based mortar: An internal curing agent for PCC. *Sustainability*, *11*(9), 2491. https://doi.org/10.3390/su11092491
58. Murali, G., & Kravchenko, E. (2026). Emerging Frontiers in Biochar-Based Cementitious Composites: Mechanisms of Carbon Capture, Integration Strategies, Economic Evaluation, and Pathways to Sustainability. *Cement and Concrete Composites*, 106503.
59. Muthukrishnan, S., Gupta, S., & Kua, H. W. (2019). Application of rice husk biochar and thermally treated low silica rice husk ash to improve physical properties of cement

mortar. *Theoretical and applied fracture mechanics*, *104*, 102376.doi: https://doi.org/10.1016/j.tafmec.2019.102376.

60. Nazar, S., Yang, J., Thomas, B. S., Azim, I., & Rehman, S. K. U. (2020). Rheological properties of cementitious composites with and without nano-materials: A comprehensive review. *Journal of Cleaner Production*, *272*, 122701. doi.org/10.1016/j.jclepro.2020.122701
61. Nejad, B. M., Enferadi, S., & Andrew, R. (2025). A comprehensive analysis of process-related CO2 emissions from Iran's cement industry. *Cleaner Environmental Systems*, *16*, 100251.
62. Olabimtan, S. B., & Damdelen, Ö. (2023). Effect of waste glass powder and recycled fine aggregate in sustainable concrete. *J. Struct. Eng. Appl. Mech.*, *6*, 343-363.
63. Olabimtan, S. B., Mosaberpanah, M. A., & Oluwole, B. O. (2025). The performance of Posidonia oceanica leaf-based biochar as a partial replacement for cement in concrete: a review of potentials, challenges, and prospects. *Discover Concrete and Cement*, *1*(1), 34. https://doi.org/10.1007/s44416-025-00034-4
64. Olii, M. R., Ali, A. Z. P. M., Djau, R. A., Doda, N., & Olii, R. S. N. (2025). Enhancing Compressive Strength of Self-Compacting Concrete (SCC) through Rice Husk Ash and Superplasticizer Incorporation. *Jurnal Teknik*, *23*(1), 229-241.
65. Oluwole, B. O., Damdelen, Ö., & Olabimtan, S. B. (2025). Valorization of industrial byproducts in concrete: synergistic effects of sewage sludge ash and silica fume with recycled plastic fine aggregates. *Discover Concrete and Cement*, *1*(1), 39. https://doi.org/10.1007/s44416-025-00039-z
66. Patel, R., Stobbs, J., & Acharya, B. (2025). Study of biochar in cementitious materials for developing green concrete composites. *Scientific Reports*, *15*(1), 22192.
67. Praneeth, S., Saavedra, L., Zeng, M., Dubey, B. K., & Sarmah, A. K. (2021). Biochar admixtured lightweight, porous and tougher cement mortars: Mechanical, durability and micro computed tomography analysis. *Science of The Total Environment*, *750*, 142327.
68. Qin, Y., Pang, X., Tan, K., & Bao, T. (2021). Evaluation of pervious concrete performance with pulverized biochar as cement replacement. *Cement and Concrete Composites*, *119*, 104022.
69. Room S, Bahadori-Jahromi A. Hydration Kinetics of Biochar-Enhanced Cement Composites: A Mini-Review. Buildings. 2025 Jul 18;15(14):2520. doi.org/10.3390/buildings15142520
70. Rupasinghe M, Zhang Z, Mendis P, Sofi M. Carbon sequestering biochar incorporated cementitious composites: Evaluation of hygrothermal, mechanical and durability characteristics. Cement and Concrete Composites. 2025 Mar 1;157:105864. doi.org/10.1016/j.cemconcomp.2024.105864.
71. Senadheera, S. S., et al. (2023). Application of biochar in concrete – A review. Cement and Concrete Composites, 141, 105134.
72. Senadheera, S. S., Gupta, S., Kua, H. W., Hou, D., Kim, S., Tsang, D. C. W., & Ok, Y. S. (2023). Application of biochar in concrete – A review. Cement and Concrete Composites, 143, 105204.
73. Shyam, S., Ahmed, S., Joshi, S. J., & Sarma, H. (2025). Biochar as a Soil amendment: implications for soil health, carbon sequestration, and climate resilience. *Discover Soil*, *2*(1), 18.
74. Sikora, P., Woliński, P., Chougan, M., Madraszewski, S., Węgrzyński, W., Papis, B. K., ... & Stephan, D. (2022). A systematic experimental study on biochar-cementitious composites: Towards carbon sequestration. *Industrial Crops and Products*, *184*, 115103.

75. Singh, Shweta, K. Ruddhra Shekaran, Rachit Agarwal, V. G. Kalpana, Humaira Athar, and Rajesh Kumar. "Enhancing the strength and durability of mixed biochar-blended mortars after Accelerated Carbonation Curing (ACC)." *Journal of Building Engineering* 100 (2025): 111743.
76. Singhal, S. (2023). Biochar as a cost-effective and eco-friendly substitute for binder in concrete: a review. *European Journal of Environmental and Civil Engineering*, *27*(2), 984-1009. doi.org/10.1080/19648189.2022.2068658.
77. Sirico, A., Bernardi, P., Belletti, B., Malcevschi, A., Dalcanale, E., Domenichelli, I., ... & Moretti, E. (2020). Mechanical characterization of cement-based materials containing biochar from gasification. *Construction and Building Materials*, *246*, 118490. doi: https://doi.org/10.1016/j.conbuildmat.2020.118490.
78. Suarez-Riera, D., Restuccia, L., & Ferro, G. A. (2020). The use of Biochar to reduce the carbon footprint of cement-based materials. *Procedia Structural Integrity*, *26*, 199-210. https://doi.org/10.1016/j.prostr.2020.06.023
79. Tan, K., Pang, X., Qin, Y., & Wang, J. (2020). Properties of cement mortar containing pulverized biochar pyrolyzed at different temperatures. *Construction and Building Materials*, *263*, 120616. , doi: https://doi.org/10.1016/j.conbuildmat.2020.120616.
80. Tee, K. F., et al. (2023). Biochar in cementitious material A review on physical, chemical, mechanical and durability properties. AIMS Materials Science, 10(3), 424-451. : 10.3934/matersci.2023022
81. Wang, Y. S., Kim, T., Lin, R. S., Li, J., & Wang, X. Y. (2024). Improved high-temperature resistance of limestone calcined clay cement (LC3) paste with biochar: Multiscale evaluation and mechanistic analysis. *Developments in the Built Environment*, *18*, 100403. https://doi.org/10.1016/j.dibe.2024.100403
82. Wu L, Farzadnia N, Shi C, Zhang Z, Wang H. Autogenous shrinkage of high performance concrete: A review. Construction and Building Materials. 2017 Sep 15;149:62-75. doi.org/10.1016/j.conbuildmat.2017.05.064
83. Yang, X., & Wang, X. Y. (2021). Hydration-strength-durability-workability of biochar-cement binary blends. *Journal of Building Engineering*, *42*, 103064. https://doi.org/10.1016/j.jobe.2021.103064
84. Yang, X., Lin, R. S., Han, Y., & Wang, X. Y. (2021). Behavior of biochar-modified cementitious composites exposed to high temperatures. *Materials*, *14*(18), 5414. **https://doi.org/10.3390/ma14185414**
85. Ye, P., Guo, B., Qin, H., Wang, C., Liu, Y., Chen, Y., Bian, P., Wang, C., Lu, D., Wang, L., Cao, Q., Zhao, W., Hong, L., Qiu, J., Gao, P., Zhan, B., & Yu, Q. (2025). Investigation of the effects of the biochar in different fractions on cement composites. Cement and Concrete Composites, 162, 106142.
86. Zeidabadi, Z. A., Bakhtiari, S., Abbaslou, H., & Ghanizadeh, A. R. (2018). Synthesis, characterization and evaluation of biochar from agricultural waste biomass for use in building materials. *Construction and Building Materials*, *181*, 301-308. doi.org/10.1016/j.conbuildmat.2018.05.271
87. Zhang, Y., Maierdan, Y., Guo, T., Chen, B., Fang, S., & Zhao, L. (2022). Biochar as carbon sequestration material combines with sewage sludge incineration ash to prepare lightweight concrete. *Construction and Building Materials*, *343*, 128116.
88. Zhao Z, El-Naggar A, Kau J, Olson C, Tomlinson D, Chang SX. Biochar affects compressive strength of Portland cement composites: a meta-analysis. Biochar. 2024 Mar 6;6(1):21. doi: https://doi.org/10.1007/s42773-024-00309-2
89. Zhou, Z., Wang, J., Tan, K., & Chen, Y. (2023). Enhancing biochar impact on the mechanical properties of cement-based mortar: An optimization study using response

surface methodology for particle size and content. *Sustainability*, 15(20), 14787. https://doi.org/10.3390/su152014787